The Study of the Forward-Voltage to Junction-Temperature Coefficient Degradation in Light-Emitting Diodes

A Thesis
presented to
the Faculty of California Polytechnic State University,
San Luis Obispo

In Partial Fulfillment
of the Requirements for the Degree
Master of Science in Industrial Engineering

By
Christopher Grasberger
June 2010

COMMITTEE MEMBERSHIP

TITLE: The Study of the Forward-Voltage to Junction-
                                    Temperature Coefficient Degradation in Light-
                                    Emitting Diodes

AUTHOR   Christopher Grasberger

DATE SUBMITTED: June 2010

COMMITTEE CHAIR: Dr. Jianbiao (John) Pan
                                    Associate Professor
                                    Dept. of Industrial and Manufacturing Engineering

COMMITTEE MEMBER: Dr. David Braun
                                    Professor
                                    Dept. of Electrical Engineering

COMMITTEE MEMBER: Dr. Lizabeth Schlemer
                                    Associate Professor
                                    Dept. of Industrial and Manufacturing Engineering

ABSTRACT

The Study of the Forward-Voltage to Junction-Temperature Coefficient Degradation
in Light-Emitting Diodes

Christopher Grasberger

Light-emitting diodes (LEDs) have recently become exceedingly popular in general lighting. As their popularity grows, the demand of more complex and more powerful systems grows as well. While optical characteristics are a crucial component of any lighting product, the main selling point of an LED is their long life and reliability. Unfortunately, the lifetime and reliability of a LED are heavily dependent on the junction temperature of the LED.

Thermal management for LEDs has become an important field study for LEDs. Unfortunately, as the LEDs grow smaller and more integrated, it becomes impossible at times to directly measure their junction temperature. When this occurs, the use of the forward-voltage to junction-temperature coefficient, or K-factor, can be used to aid in measuring the junction temperature. Often the K-factor value is quoted as a constant, even while the rest of the LED degrades.

This thesis explores the use of the K-factor and attempts to determine if there is a significant change in the K-factor due to degradation. To test this, a custom data acquisition system was built. Two test groups were thermally aged and periodically recalibrated to detect any changes in the K-factor. At the end of the 3000-hour test, one board had failed due to degradation, while the second board did show a statistically significant change in the K-factor; which was slightly more than 10%.

ACKNOWLEDGEMENTS

TABLE OF CONTENTS

LIST OF FIGURES

LIST OF TABLES

Chapter 1 - Introduction

In the last few years, light-emitting diodes (LEDs) have begun to grow in popularity for general lighting. The claim of greater efficiency and no toxic chemicals, such as mercury, has drawn a great number of customers to the market. This growth of customers has also driven many companies to research LEDs and further the technology.

Originally LEDs were used mostly as indicators. The recent demand of LEDs in general lighting applications such as streetlights and indoor lighting, has created a huge push to increase the amount of light being output from the diode. An example of a newer LED technology for general lighting is the Philips LUXEON Rebel, shown in Figure 1.1. In order to compete with current lighting technologies such as fluorescent tubes, the LED market has to constantly improve the light output of each LED.
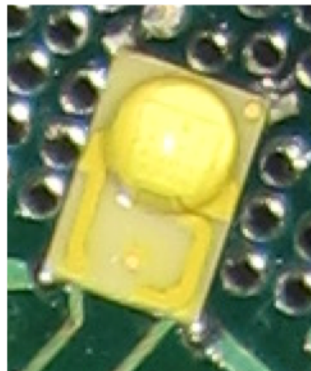
**Figure 1.1: Philips
LUXEON Rebel**

There are two groups attacking the problem of light output. First, the fixture designers have been packing more and more high-powered chips into small areas to get increased overall light output. The other group is the chip manufacturers. Cree, for example, recently announced that they had broken the 200 lumens per watt barrier [1].

While the chip manufacturers make designers' jobs easier by making each chip work more efficiently, the designers are always pushing the LED chips to their maximum to keep a competitive edge. Even though LEDs are extremely efficient compared to incandescent bulbs, they are not perfect by any means. In fact, most of the power that is put into the diode is still dissipated as heat instead of light output. Also, in contrast to incandescent tubes or halogen bulbs, LEDs do not operate well at high temperatures.

High LED junction temperatures are detrimental in many ways. The first, and most obvious, way that high temperatures can damage an LED is by decreasing its light output permanently. When an LED's light output reaches a certain percentage, typically 70%, the diode is considered to have "failed." Also, high temperatures will tend to cause the diode chip itself to emit a slightly different wavelength of light, which results in a shift in color. Finally, white LEDs use a coating of phosphor on top of a blue LED to emit white light. This phosphor is very sensitive to heat and will degrade rapidly which also causes the light output to change colors. Since heat is so detrimental to LEDs, there is a need for thermal management and characterization of this heat output.

In order to characterize the thermal management solution for an LED product, there needs to be a method to measure temperatures. This thesis analyzes the use of a common way to measure LED junction temperatures via the diode's forward voltage and then attempts to determine if this method works as the diode degrades.

Chapter 2 - Literature Review

2.1 Thermal Management

Thermal management is a huge part of the LED lighting market. According to Cree, a majority of LED failure mechanisms are temperature dependant [2]. Also, thermal management is a key technology for creating reliable, high lumen, LED systems [3]. While thermal management is critical for every LED product, it is often difficult to analyze the thermal characteristics of a product. Since LEDs can last upwards of 100,000 hours, active components such as fans are not an option, as the moving parts of a fan would fail long before the LED does. Additionally, an LED is considered to have failed if it reaches 70% of its initial light output [4]. In fact, Energy Star, a Department of Energy group, requires that luminares used in commercial applications must maintain at least 70% of initial lumens for 35,000 hours [5]. Luminaire manufacturers shall adhere to device manufacture guidelines and test procedures for thermal management [5]. Beyond the requirements of the government and chip manufacturers, Underwriters Laboratories, commonly called UL, enforce that a fixture surface exposed to being touched may not exceed 90C [6] as one of many criteria to receive their safety approval.

Since LED products are now being heavily regulated for safety and quality, it is the job of the thermal engineer to ensure that the chips do not overheat. Each chip manufacturer attempts to help the problem by using an innovated packaging mechanism. Philips LumiLEDs, for example, uses Gold-Gold Interconnects (GGI) [7] to improve thermal performance of their packages. Additionally, the chips can be directly mounted to the heat sink as shown in Figure 2.1. Once the heat is conducted to the heat sink, it

must be able to transfer thermal energy from the solid to the ambient air. This is called

convection, which is composed of two mechanisms: diffusion and bulk fluid motion, [8] or

in other words non-stagnant air. Additionally, there is radiation, which can be extremely

complicated. Radiation does contribute to the dissipation; however for the sake of simple

models, it is sometimes ignored. The input power from the LEDs, the heat sink, and the

moving air all are highly variable from design to design. In order to characterize this,

properties of the problem must be understood.
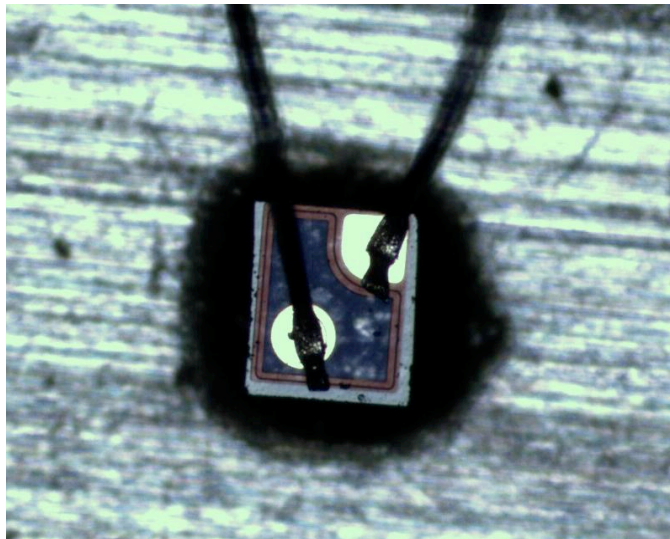
Figure 2.1: Photograph of an LED that is 235x275x90µm with wire bonds.

Thermal analysis of basic fixture designs can be modeled as a resistor network.

Where temperature is analogous to voltage, input power (Watts) is analogous to current,

and thermal resistance is analogues to electrical resistance [8]. Figure 2.2 shows how a

fixture with a single LED and a heat sink can be converted into a resistance model. Once

the model has been developed, values need to be determined. The ambient air

temperature can typically be easily measured. The input power can be determined as

well and the thermal resistance of the LED package is specified in the datasheet (R_{LED} in

Figure 2.2). However, this still leaves three critical values that cannot be determined

easily. The first is the thermal resistance of the heat sink, second is the convection coefficient, and the last is the junction temperature of the LEDs. If the junction temperature could be measured, the thermal resistance of the heat sink and convection coefficient could be lumped together which would give insight into the effectiveness of the heat sink design.
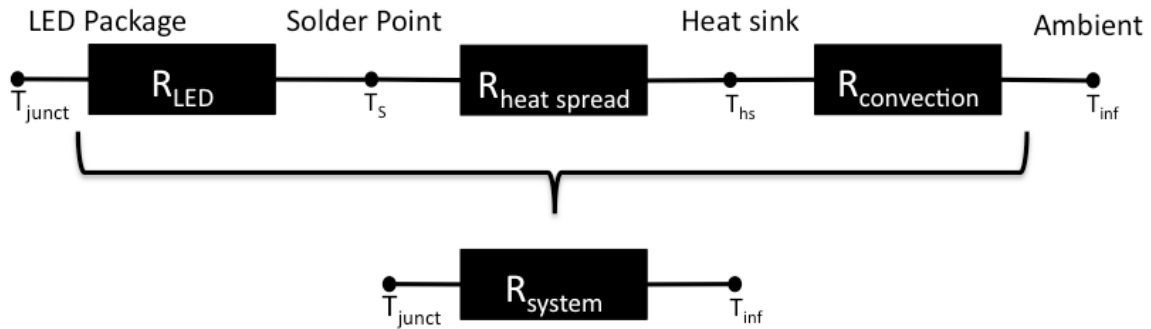
Figure 2.2: Example of a thermal resistance network for a single LED

The junction temperature of an LED is critical because this is the junction between the positively doped region and the negatively doped region. When the electrons begin to flow across the device, there is a voltage drop across the gap. As the energy crosses the gap light is emitted, but also heat is emitted. This region can be very small and often the junction is covered by a lens or phosphor. To use a thermocouple would be ill advised on the junction because the probe would measure the local air more than the junction. There are a myriad of ways to measure a LED's junction temperature. However, a relatively simple and accurate way to measure the junction temperature is to use the forward voltage of the diode.

2.2 Forward Voltage Temperature Measurements

A relationship between the forward voltage of a diode (not just LEDs) and the junction temperature of a diode exists. While it is unclear if it is the average temperature of the junction or if it is the maximum, it still gives a measurement of an otherwise difficult value to measure. Some additional complexities exist; however this process is fairly well understood and is used in other industries.

The use of the forward-voltage to junction-temperature coefficient (or K-factor) has widely been used in the thermal characterization of heat sink solutions for CPUs. A simulation chip package, the size of the CPU, is built with one or more diodes in the package. The desired amount of power is applied to the package via a power resistor or the test diode itself. Using the diode as a temperature measurement, the characterization of the heat sink design can be performed.

If one looks at the ideal diode equation there is a correlation between the current (J), voltage across the diode (V_D), and the temperature (T). Values for q (charge of an electron) and k (Boltzmann constant) are constants. The ideality factor (n) is typically in the range of 1 to 2; however to fit this model to a LED like the LUXEON Rebel, the value is closer to 3, which exceeds the expected range. Equation 2.1 shows the equation, which is also known as the Shockley Ideal Diode Equation.

$$J = J_s \left(e^{qV_D/nkT} - 1 \right)$$

Equation 2.1: Shockley Ideal Diode Equation

If Equation 2.1 is reorganized, and J_s is assumed to be approximately constant, then a simple derivative of diode voltage with respect to temperature can be taken. Equation 2.2 shows the result of this simplified equation.

$$\frac{dV_D}{dT} = nk \ln\left(\frac{J}{J_S} + 1\right)$$

Equation 2.2: Derivate with respect to time of Shockley Ideal Diode Equation to show current dependence on K-factor

While Equation 2.2 does not include all of the detail of the saturation current (J_S), it does show how the current being applied to the diode does play a role in the value of the K-factor (dV_D/dT).

Equation 2.2, as mentioned previously does not account for the dependence on temperature in the saturation current. While there is a degree of dependence, it is not terribly significant. The equation that describes the saturation current is shown in Equation 2.3. This equation is taken from the JEDEC (formerly known as Joint Electron Devices Engineering Council) standard for electrical temperature measurement [9].

$$J_s = M * T^m e^{-V_{G0}*q/nkT}$$

Equation 2.3: Equation to express the saturation current [9]

Since the K-factor (or dV_D/dT) is not significantly temperature dependant, the JEDEC standard states that a change in voltage multiplied by the K-factor results in a change in temperature or Equation 2.4 [9]. Y. Xi and E. F. Schubert also state that experimental V_f versus T relationship is very close to linear and can be fitted by Equation 2.5 where T_0 is the oven temperature and A and B are fitting parameters [10]. The B fitting parameter is also the K-factor.

$$\Delta T = (\text{K-factor}) \text{ x } \Delta V_F$$

Equation 2.4: K-factor equation recommended by JEDEC [9]

$$V_f = A + BT_0$$

This measurement system is widely used and many expensive tools have been developed to measure the K-factor for testing. Unfortunately, LED chip manufacturers do not specify how this property degrades over time. It is very well known that optical properties and other properties, such as internal resistance, will change over time. It would therefore not be unreasonable to hypothesize that the K-factor will also change as the LED degrades. According to LumiLEDs, it does change as the LED degrades. However, there is no research available to the public to this author's knowledge.   Since there is a lack of data available on this topic, my thesis is to determine if there is a significant change in the K-factor during degradation.

Chapter 3 - Experiment Design

In order to collect data to test the hypothesis, two distinct stages were required. First, a data acquisition system capable of measuring the K-factors was required. Second, the physical data collection was required.

3.1 Data Acquisition System

The development of the data acquisition system (DAQ) was an enormous undertaking on its own. Fortunately, the requirements, designs, and testing procedure developed for this thesis had begun long before the topic was ever chosen with the intention of building a commercial handheld tool. The following sections give a brief outline of the design process for the DAQ. Detailed descriptions of components can be found in Appendix A.

3.1.1 Requirements

Like any project or system, there are a number of constraints that must be all solved at once. This DAQ was no different. Unfortunately, to enumerate all of the requirements for the data collection system would result in a report on its own. However, this project, like any other, has a few notable ones that will be elaborated on. Measuring a LED's K-factor requires a rapid activation and measurement to avoid self-heating of the

diode. This requires a high speed switching system to turn on and off the LED. Additionally, the analog-to-digital converter (ADC) must be quick enough to gather samples during the time the LED is on. Also, this DAQ must be able to calibrate a diode over a large range of currents and handle multiple LEDs.

The longer a diode is left on, the closer to a steady state temperature it will become. However, when calibrating a diode, it must be calibrated with as little internal heat generation as possible. This is done so that the measured data point is effectively the oven temperature. This problem is compounded by the fact that in order to measure a forward voltage across a diode, the diode must be energized. While the voltage only varies slightly, there is a large range of currents that can be applied to the LED. Considering the worst-case input power condition, which is 1A for the LEDs being tested, an estimation of a maximum pulse length can be obtained. This results in a value around 200 microseconds before the internal heat generation becomes noticeable.

In conjunction with high speed switching, a high-speed data acquisition system is required. A speed on the order 1 million samples per second was required so that a reasonable amount of data can be collected on the diode before it is turned off. There is a tradeoff between speed, accuracy, and cost. At a minimum, 16 bits is required to get reasonable resolution at 1mV with a 5V reference. Ideally, 18 bits would be desired. Also, the analog-to-digital converter (ADC) selected to do this measurement must be simple enough that the entire project is not delayed due to the details of implementing the ADC.

The system also must be able to measure various currents since the forward-voltage to junction-temperature coefficient (K-factor) is dependent on current (see

Equation 2.2). The testing of many currents would be useful as the diode may possibly degrade differently with different currents. Many single-chip high-brightness LEDs have a maximum operating current of 1A. Running anything at its maximum current for long periods time, whether it is an LED or LED driver, may cause damage to the component. Therefore this system must be able to handle 1A for long periods of time in the event it needs to drive a LED instead of simply pulsing it. Additionally, it must be able to handle lower currents such as 20 or 100mA to ensure a wide measurement range.

Finally, the DAQ must be able to measure multiple LEDs to collect data faster. It is impractical to repeatedly open the oven to rewire the LEDs. Each time the oven is opened; there is a long wait to allow the oven to return to a steady state temperature. This creates the requirement of interfacing at least eight diodes at once.

3.1.2 Design

The final data acquisition system design consisted of integrating a National Instruments M-Series PCI Card (model #2654), LabView 8.6, and a custom designed interface board. LabView was selected because it would allow for rapid development of a graphical user interface (GUI) and the interface with the PCI card. Alternatively, the PCI card could have been interface with DAQMX, which is a compilation of C++ libraries. However, based on time constraints, learning how to use the DAQMX libraries possibly could have been slower than using LabView. The PCI card that was selected was chosen because it was available for student use. Finally, the interface board was designed to address the issue of high speed switching. LabView, on its own, is not

capable of switching an LED on and off, and also collecting data quickly enough through

the PCI card. A few proof of concept tests were performed and it was found that to turn a

LED on, collect one sample of data, and turn the LED off took a total of 10 milliseconds.

The longest that an LED should stay on for the collection of data is about 0.2

milliseconds. By using an interface board, it was possible to handle the switching while

letting the PCI card collect the data at a high speed.   Figures 3.1 shows how LabView

interfaces with the PCI card, microcontroller, and the LED.
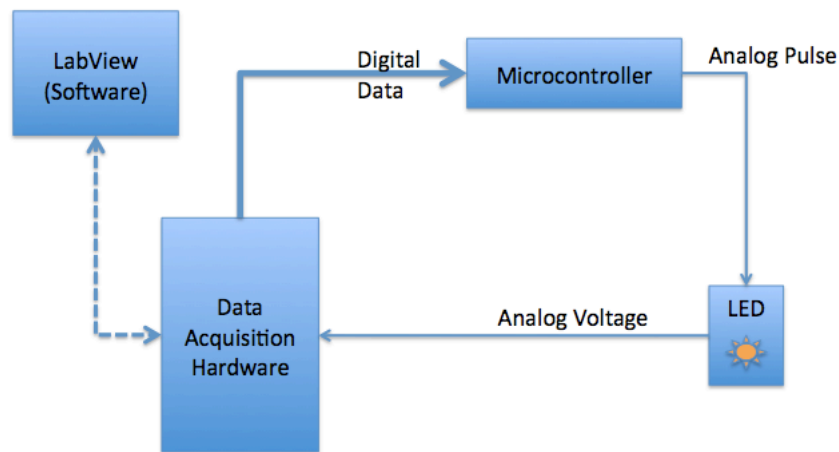
Figure 3.1: Graphical overview of system.

High speed switching is handled by having LabView send a pulse to the

microcontroller. The microcontroller has a short delay (programmed currently to ¼

second), and then the microcontroller enables an analog switch. During this delay,

LabView can switch modes to data collection. After the switch is enabled, the analog

switch sends a voltage to an operational amplifier, which acts as a constant current driver.

When the analog switch is not enabled, the output voltage is zero which results in no

current through the diode.   Figure 3.2 shows how the analog switch is connected to the

op-amp, which is acting as a constant current driver.   After a preselected time, the analog

switch is disabled automatically by the microcontroller.
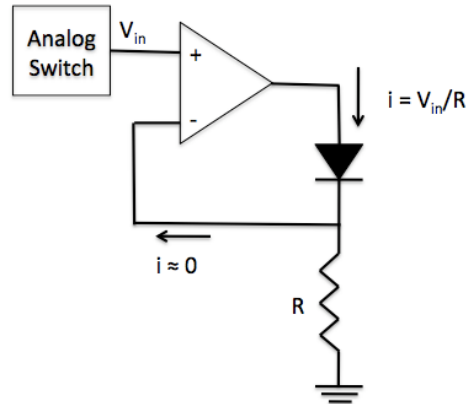
Figure 3.2: Simplified circuit of constant current LED driver

The design uses the PCI card to handle the analog-to-digital conversion. This was done to speed up the design and verification process because the PCI card was verified to be working at the factory (and recently for another student's thesis). The PCI card is able to collect 1.25 million samples per second, which worked out quite well for this application. Within a 200-microsecond period, 250 samples can be collected. During some initial testing, it was found that the op-amp was marginally stable when operating. A few modifications were added to stabilize the circuit. The oscillations were damped out significantly, however the rise time was slowed. The rise time went from about 1 microsecond to 50 microseconds. Losing 50 microseconds out of the original 200 is a sizeable amount of data. To compensate for this, samples were taken for 440 microseconds (550 samples) and a linear model was fitted to the collected data. This model was done so that ideally the intercept along the vertical axis would be the forward voltage at time zero. Figure 3.3 shows how a linear fit would be applied to a 700mA pulse test of a diode. While a linear fit does not describe all of the physics, the concept was developed assuming the LED is heating uniformly across the junction surface.
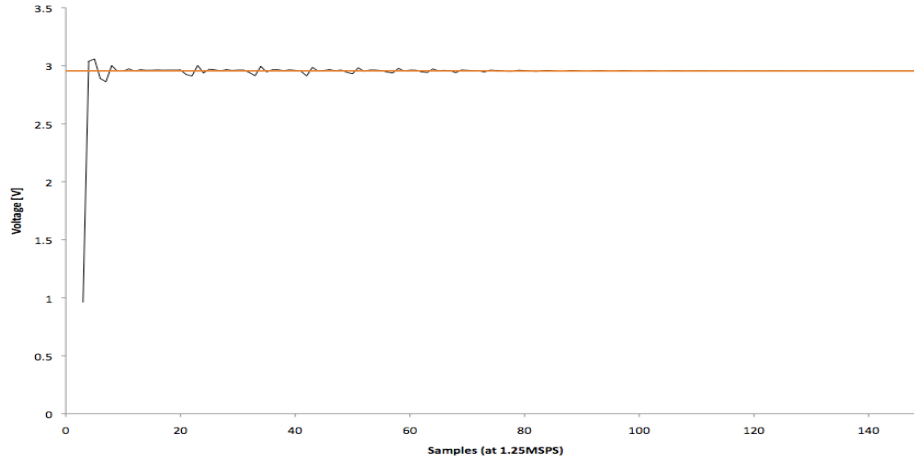
Figure 3.3: Linear trend line overlaid on data to show intercept.
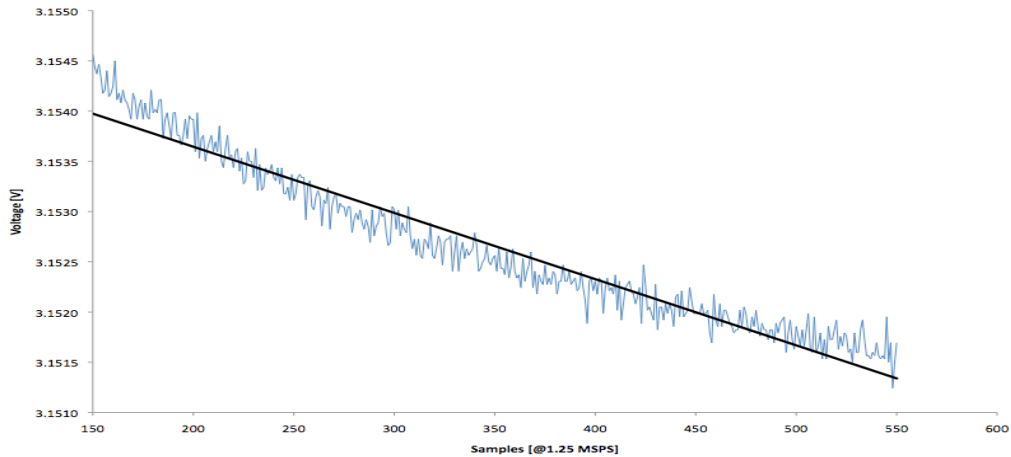
Figure 3.4: Discrepancy in linear trend line and data used for intercept estimation.

Figure 3.4 shows a close up of the data past the initial rise time. The linear trend lines use data from the 150th data point until the 550th data point. This gave sufficient time for voltage to stabilize. There was a substantial overshoot, which was avoided by starting at the 150th data point. While a first order approximation is not perfect, it gives a better estimation of the data point than a simple average of all of the collected samples. It should be noted that in the 100mA and 350mA test current pulses, the data is nearly linear and horizontal when plotted due to very little self-heating.

Finally, the design incorporated numerous double-throw double-pole (DPDT) relays to handle multiplexing and current range selection. There were 16 DPDT relays that were dedicated to multiplexing up to eight diodes. Each diode had two relays dedicated to allow for separate powering and/or testing of LEDs. This was done so that an external power source could be used, or simply use the DAQ as a constant current LED driver for long durations without measurement. The choice to use relays over multiplexers for the LEDs and resistors was to accommodate high current pulses. Many multiplexers within the project's price range had a maximum current of 800mA. The use of relays allowed upwards of several amperes.

Relays were also used to address each current sensing resistor separately. There is one for each of the following: 0.25Ω, 10Ω, 100Ω, $1k\Omega$, $10k\Omega$, $100k\Omega$, and $1M\Omega$. However, due to limitations on addressing from the PCI card, only 0.25Ω, 10Ω, 100Ω, and $1k\Omega$ were used. These resistors allowed for the following current ranges: 1000-100mA, 100-10mA, 10-1mA, 1-0.1mA current ranges respectively. Issues with relay contact oxidation were addressed in three separate ways. First, the relays that were selected are resistant to oxidation build up. Second, the LabView user interface only switches contacts when there is no current across the contacts. Finally, measurements of the diodes are made using 4-wire measurements which nearly negates all resistance build up [12]. Figure 3.5 shows how in 2-wire measurements, the resistance of the test leads can add error; and how in 4-wire measurements, the test leads do not affect the measurement. For detailed descriptions of components, PCB layouts, and images refer to Appendix A.

Current Source

$i \rightarrow$ R_{Leads}

Voltmeter

R_{Load}

R_{Leads}

2-Wire Measurements

Measured Voltage = $i*(R_{Load} + 2*R_{Leads})$

$i \rightarrow$ R_{Leads}

R_{Leads}

$i \approx 0$

Voltmeter

R_{Load}

Current Source

R_{Leads}

R_{Leads}

4-Wire Measurements

Measured Voltage = $i*(R_{Load})$
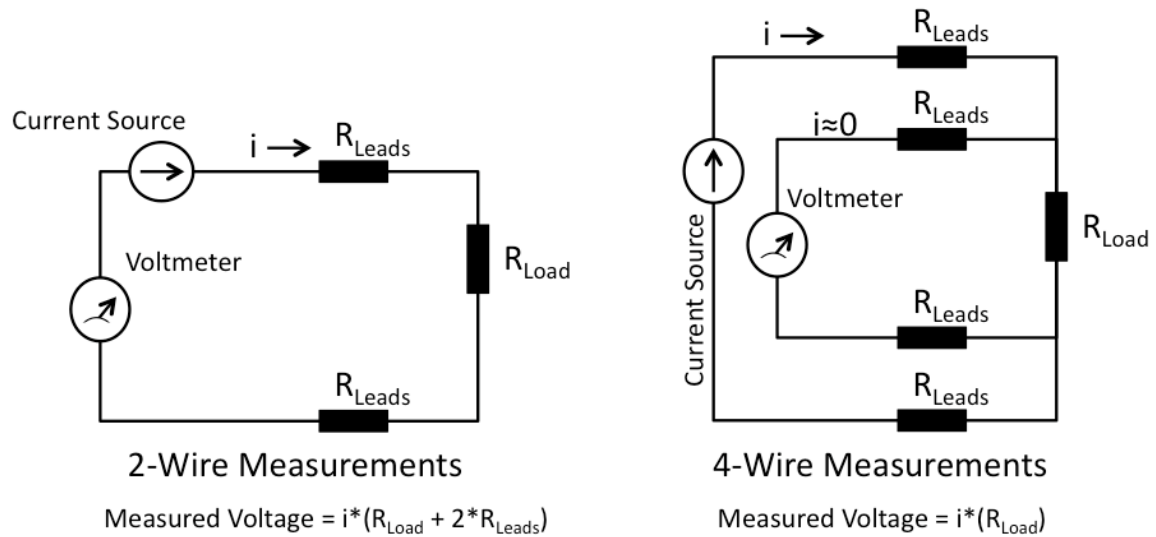
Figure 3.5: 2-wire versus 4-wire measurements.

3.1.3 Fabrication

The design of the PCB schematic and layout was done in DipTrace[1] with a personal license. The Gerber files generated by DipTrace were sent to Advanced Circuits in Colorado for fabrication. The components were ordered from Digikey (see Appendix A.3 for Bill of Materials). Ultimately, two revisions were fabricated. Each board cost approximately $260 between components and board fabrication. All components were hand soldered, including both surface mount (SMT) and through-hole (THT) components. Figure 3.6 shows the final revision of the circuit board mounted in the chassis.

---

[1] www.diptrace.com

Figure 3.6: Final revision of the interface board in the chassis.
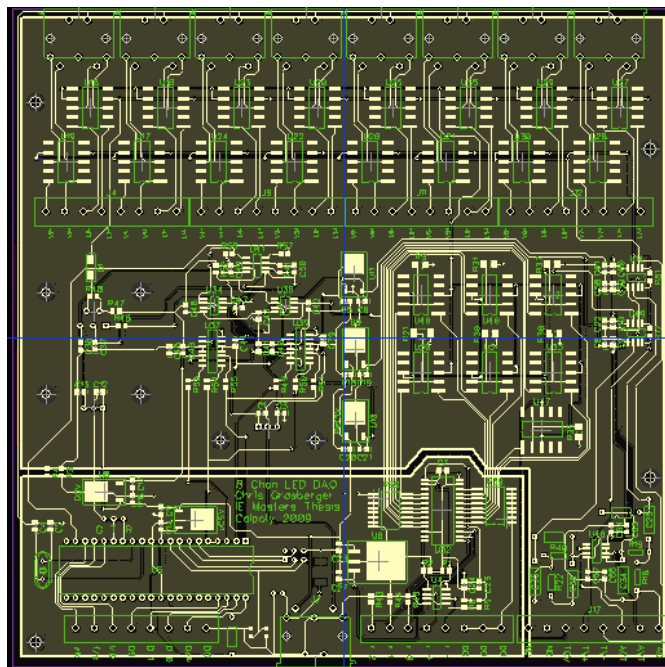
**Figure 3.7: Screen capture of DipTrace showing the top layer of
the PCB layout used in DAQ interface.**

The first revision identified several design flaws including incorrect hole sizes for through-hole connectors. A few logic errors were identified and resolved by fabricating a second board.

The second board (layout shown in Figures 3.6 and 3.7) is the board that was used to collect all of the data for this thesis. While hole sizes were fixed, there were still a few

logic errors in the same place as before. To resolve this, many modifications were made to the resistor multiplexing, which is why only four resistors are used instead of all seven.

After each component was soldered on, it was tested for functionality and tested to verify it affected the circuit correctly. This was done off campus. This allowed for the development of the microcontroller code without bringing all of the components to campus. A couple weeks of working on the microcontroller code was required to test the board with simulated inputs to verify its outputs. After the board was verified as much as possible remotely, it was taken to campus to build a chassis and connect it to the PCI DAQ Card; and then ultimately LabView.

With the assistance of Jason Maynard, we assembled a three-piece chassis. This was done because there are critical test points on both sides of the circuit board. By having the circuit board attached to the middle part of the chassis and having two removable covers (top and bottom), it was possible to test the board with minimal difficulties. See Appendix A.5 for an assembly of the chassis. Figure 3.8 shows a view down from the top of the PCB and chassis with both covers removed.
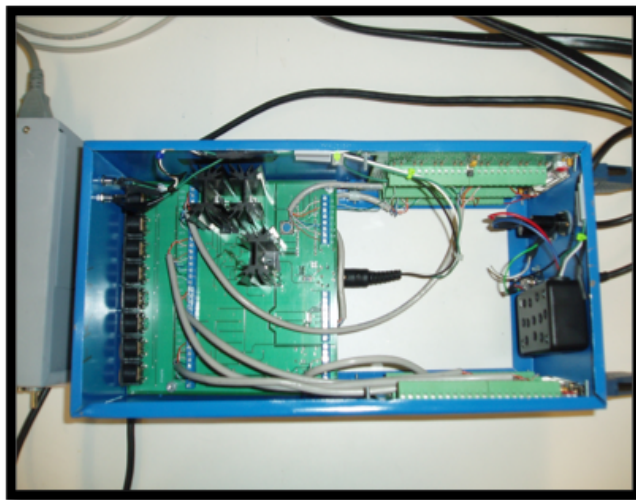
Figure 3.8: Bottom of interface circuit board showing heat sinks.

18

Inside the chassis were two breakout boards (they are mounted vertically, see Figure 3.8) that connect to the PCI card DAQ. These breakout boards allowed all 68 possible connection points via screw terminals to be addressed. Using twisted pairs inside of insulation (simply for organization as this insulation is not shielded) the breakout boards were connected to the interface PCB board. Holes were drilled into the front of the chassis for LED power indicators and diode connection sockets. The back holes were made for power input and fuse replacement. Additionally, there were two slots placed on the back so that the custom National Instruments plugs could feed through and connect to the breakout boards. Finally, the chassis was painted. A small modified chassis was also built for a computer power supply to make a dedicated power supply for the DAQ. The power supply is the grey box to the left in Figure 3.9.

Figure 3.9: DAQ Interface with power supply.

Next, the LabView interface was built up. Jason assisted a few times on the development with the interface by verifying the connections between the PCI card and the interface board; however no assistance was required for everything else described in the following sections.

3.1.4 Interface

In designing the LabView interface, there were numerous false starts. These false starts occurred because it appeared that the DAQ was ready to collect data, but after starting to collect data it became apparent that it was too slow to feasibly collect one set data, let alone several sets of data. Initially only software drivers were made to run the interface board. These were controlled by toggle switches in the interface. Using these toggle switches proved to be extremely slow and this prompted the development of controls, which could automate the slower steps. In doing this, it reduced the collection time of one data set from 80 hours to 30 hours. Another set of controls was later added which reduced the collection time down to 10 hours. The interface was never designed to be used for anything but this research topic, so organization was not planned ahead of time; however in the end, the critical components are in a light blue and neon green backlit section of the interface shown in Figure 3.10. These critical controls allow the user, to select the desired test current, desired oven temperature, and then push "Process Board." The system then performs all of the required steps to measure all of the LEDs connected to the DAQ. While this device does not directly control the oven, it will not collect data unless the temperature is within ±1°C of target temperature. See Section 3.2.2 for a test procedure to operate the system.
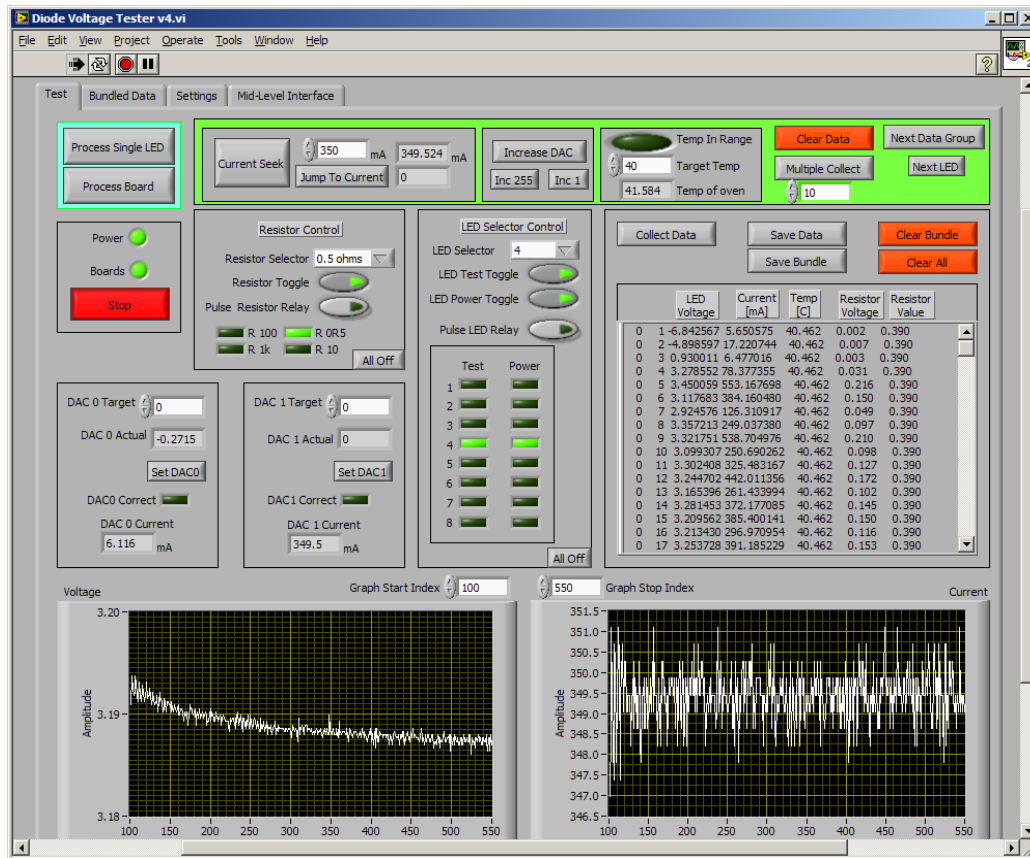
Figure 3.10: Graphical user interface developed in LabView to run the data acquisition system.

The interface also allows control over which resistor and LED is being used. While these processes are automated, within the green backed regions of the interface, they can manually be controlled as well. There is also a region to the right that shows the collected data in list format. The GUI allows for the list to be saved, cleared, or bundled[3]. Two other notable parts of the main interface are the two plots at the bottom of the screen. These show the data from the last pulse. They are useful in identifying problematic LEDs. In Figure 3.10 current plot looks unstable, however looking more

---

[3] Bundling is where the GUI takes the data and puts it into a set of columns of data. Each set of data has the sample number, voltage, current, temperature, and other values. When these are bundled, it takes all of these values (which are stored in columns) and places them in a matrix with other columns. So if each set of data is 5 columns, then if three sets of data are bundled, there will be 15 columns of data when viewed in Excel.

closely at the vertical axis, the variation in values are within an acceptable tolerance and the average is within 2% of the target current.

Near the top of the screen, there are a group of tabs to other parts of the interface. One tab allows the user to view the data that has been bundled together. This is useful for checking that all of the LEDs have been measured and to visually verify that the values seem reasonable. There is also a tab to set options relating to timing and thermocouple offsets. Finally, a less used tab shows some of the low-level software drivers that have been incorporated into many of the controls on the main interface. These low-level drivers are used a great deal without the user's knowledge. See Appendix A.3 for screen shots of these tabs.

3.1.5 Verification and Calibration

To use this device as a tool, it first had to be calibrated. In doing the calibration, several things were verified and others were identified to be problems. This section is closely tied to the fabrication because testing was done during assembly. A few important things were specially calibrated at the end, which are: forward-voltage to temperature coefficient (K-factor) accuracy, voltage measurement accuracy, speed of measuring, and resistance value of current sensing resistors.

The K-factor verification was actually performed last, however since it is so relevant to the subject, it is presented first. To verify the accuracy during the initial calibration of the LEDs, an average was taken of their K-factors at each corresponding current. This average was composed of 37 LEDs (40 were soldered, but 3 failed). They

were then compared to the datasheet provided by the manufacture. The results showed an identical match to the datasheet as shown in Figure 3.11.
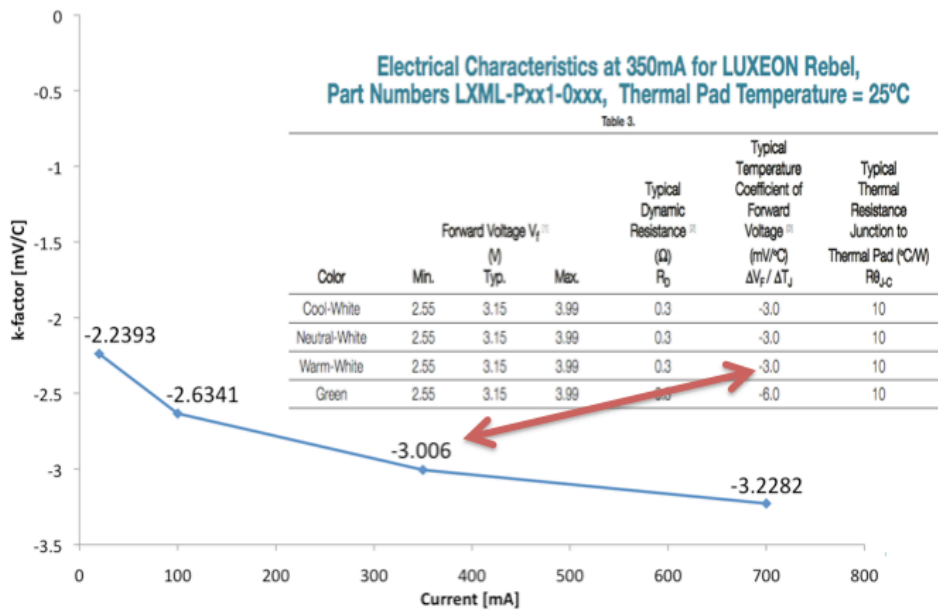
Figure 3.11: Comparison of LUXEON Rebel datasheet with collected data.

The accuracy of the voltage readings from the PCI card was also verified. While these values were quoted to be accurate in the datasheet, it was necessary to verify that the measurement device had not been damaged.   Voltages measured by the DAQ were compared against an Instek GDS-1062A oscilloscope when both the DAQ and oscilloscope measured a steady 1 VDC output. The PCI card measured 10 samples and averaged them. These were then compared to the measured value from the oscilloscope. There was less than a 0.5% difference in values. It was also measured against a Fluke 289 multimeter with similar results. These tests confirmed that the PCI card DAQ was accurately measuring the voltages.

The speed of measurements was important to simply know if the system was actually capable of high-speed measurements. To test this, a function generator generated a 1kHz square-wave signal. The number of samples measured by the DAQ

during the high state was counted. An oscilloscope verified the frequency of the signal. The results of this test showed that it was measuring at 1.2 million samples per second.

Finally, the resistance value of the current sensing resistors was verified. The components were selected to have very little variation in resistance due to temperature changes. Additionally, all resistance values, except the 0.25Ω, were specified to be accurate to $\pm0.1\%$. The resistance values, other than 0.25Ω, were verified by using a fixed DC output power supply. A Fluke 289 multimeter measured current while the PCI DAQ card measured voltages. The current applied to each of these resistors was selected so it would not violate their maximum rating but still allow for both measurement devices to measure in their most accurate ranges. These resistors were verified to fall into their specified $\pm0.1\%$ tolerances. The 0.25Ω resistor required special treatment.

The 0.25Ω resistor was tested after being soldered on to the board and the interface board was connected to the PCI DAQ card. Once it was in place, a DC power supply was connected to the resistor through one of the diode channels. A Fluke 289 multimeter was then placed in line to measure the current. The physical measurement of the voltage across the 0.25Ω was measured by a differential op-amp with a unity gain. This op-amp output its voltage as a pseudo-differential signal, which was then measured by the PCI DAQ card. Using the average of measurements from both the multimeter and DAQ the resistance of the 0.25Ω was measured. It measured to be 0.37Ω, which includes the resistance from traces. The physical chip had a $\pm1\%$ as specified by the manufacturer. The correct value was programmed into the interface and is accurate to $\pm0.5\%$ based on the error from both the multimeter and DAQ. While this is not as accurate as the other resistors, it is still sufficient.

3.2 Data Collection

This thesis requires the collection of data that could be turned into a forward-voltage to junction-temperature coefficient, K-factor, and then this data was used to determine if the K-factor degrades over time. To design this test, several factors were considered: First, how would the K-factor be measured? Second, how could the test remain practical without require an absurd amount of equipment? Finally, how could multiple levels of operation be introduced into the study?

The K-factor is constant for a given current at a specific time. In order to calculate a given K-factor value, at least two data points must be taken at a fixed current. Ideally, these points should be at very different temperatures. EIA JEDEC standard recommends a minimum of a difference of 50 degrees [9]. To ensure that one of these data points was not corrupted by measurement errors, five temperatures were measured in this study: 20°C, 40°C, 60°C, 80°C, and 100°C. While this took substantially longer to collect this data, it allowed for better verification of the data. By using a linear trend line on the data, the data could be used to verify that there were no outliers or measurement errors. Additionally, the slope of the trend line would be the K-factor. See Figure 3.12 for a plot of typical data collected from a LED and the trend line showing the K-factor. By using five temperatures, any outliers would become apparent, as the data would not fall on the line.
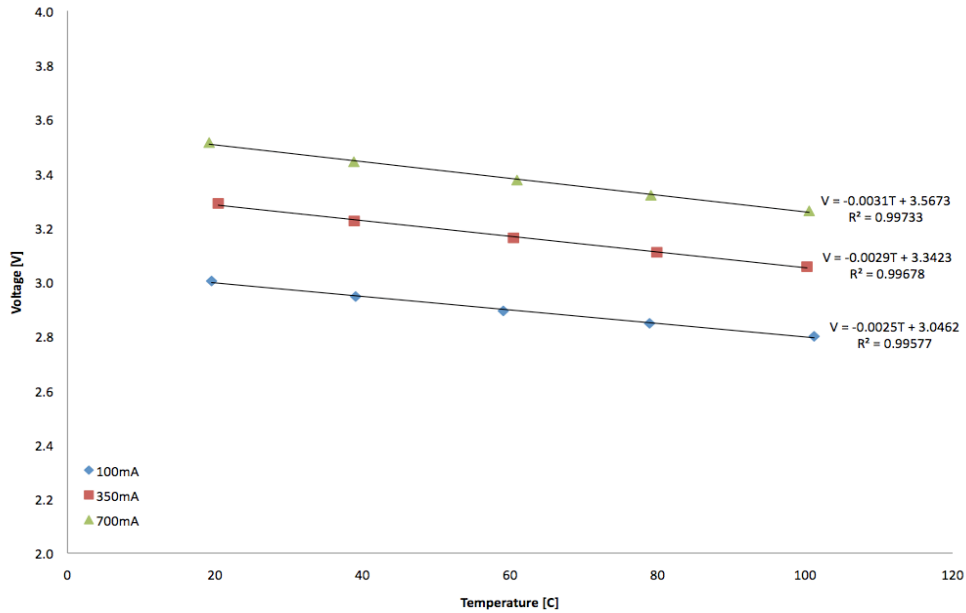
Figure 3.12: Example of collected data with linear trend lines.

Since LEDs can last a very long time, the tests must be accelerated in order to see

results in a practical amount of time. LEDs degrade rapidly at high temperatures and thus

using high temperatures would be a practical approach to accelerating the tests. There

are two obvious ways to heat a LED up to high temperatures. One would be increase the

current, which is ultimately increasing the input power. The second is to raise the

temperature of the ambient conditions. The problem with increasing the current is that as

more current is put in, the temperature will rise accordingly for a set thermal solution.

Alternatively, a set current could be used with multiple ambient air conditions to raise the

junction temperature. Unfortunately, multiple ovens would be required non-stop during

aging. It should be noted degradation from high junction temperature due to ambient

conditions might be different from high junction temperatures due to high currents [13].

Since there was a limitation on resources available, only the current approach was used.

Two currents were selected, which ultimately determined two junction-

temperatures. One temperature was designed to be very high, near the maximum

operating conditions or higher; the second was high, but at least 20-30 degrees cooler so that degradation would not be nearly as fast. The goal of this was to ensure that if the lower temperature did not show any results, possibly the higher temperature did. Similarly, if the higher temperature LED degraded too rapidly, the lower temperature would at least have some data to show. Also, there was to be a control board, which was never operated. The currents were selected after the initial data collection. This was done so that a thermal resistance could be determined from the junction temperature to the ambient air. This allowed for currents to be selected that would allow specified average junction temperatures. While the thermal resistance did vary, they were grouped into like averages. This formed two groups: A and B. Group A was aged at 470mA which put the junction temperature at 145°C on average. Group B was aged at 350mA which resulted in an average junction temperature of 115°C. The maximum operating temperature for the LEDs according to their datasheet is 150°C. See Figure 3.13 for an overview of the groupings.
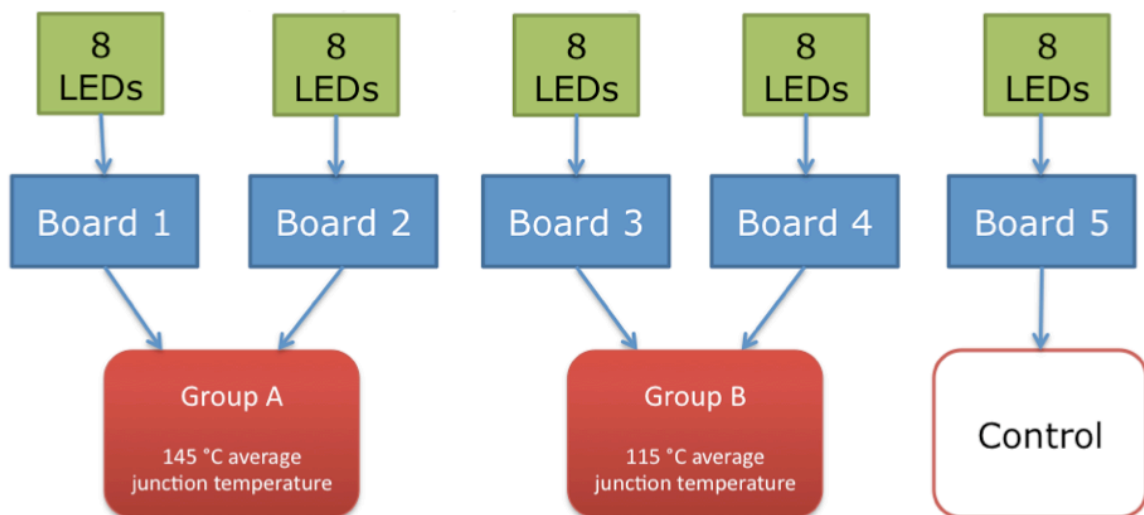
Figure 3.13: Plot of how the LED groups were formed.

As shown in Figure 3.13, there are five boards to test. The DAQ system was designed to handle eight LEDs without having to opening the oven and rewire for new LEDs. Having multiple replications per aging current level (Group A and B) would help to gather better data. It was decided to use 16 LEDs per level, and 8 for a control test. All 8 LEDs were put in series so that they would receive the exact same aging current. Constant current drivers were used for both Group A and B. Drivers from Thomas Research Products were used for both groups. Group A used a 350mA driver, TRP model TWC-030S035SS; and Group B used two 470mA drivers, TRP model LED17W-36-C0470. All drivers are regulated to within ±1% of nominal value. Figure 3.14 shows how the LEDs were connected to their corresponding drivers.
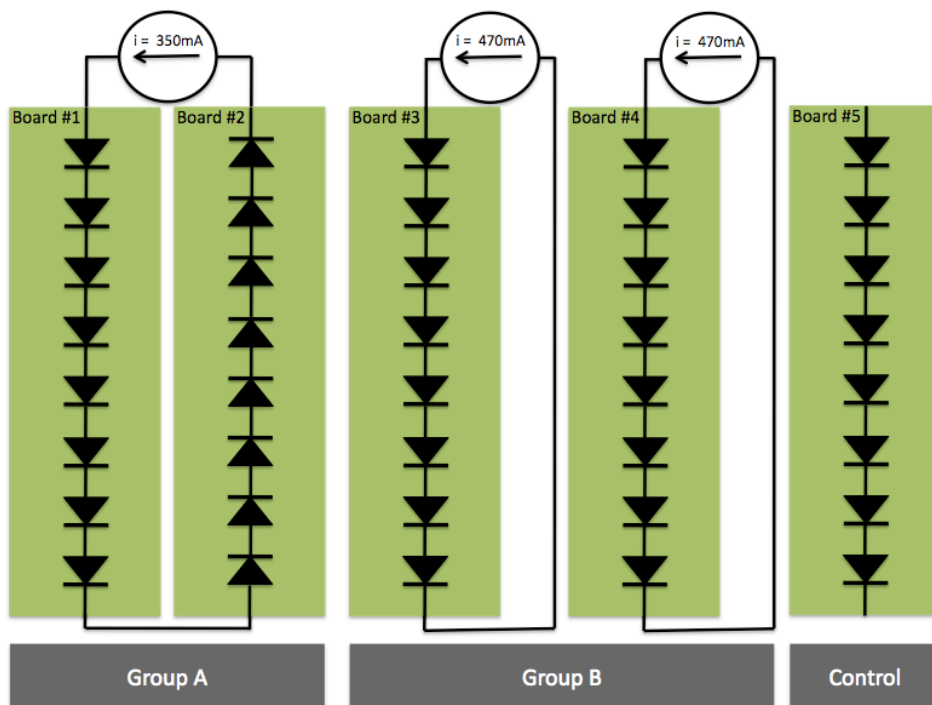
Figure 3.14: Circuit diagram of LEDs while aging.

3.2.1 Test Vehicle Design

After the number of LEDs to be tested had been determined, then a way to mount all of the LEDs was needed. The requirements for the design required that no LED received a different thermal condition than another. This was done so all LEDs could be considered to have aged identically. Numerous layouts were considered, but in the end a circular shape with equal spacing between LEDs was selected. This shape allowed for thermal symmetry between LEDs. This meant that each LED affected the nearby chips equally so the net effect was zero. Figure 3.15 shows the first revision of the PCB.
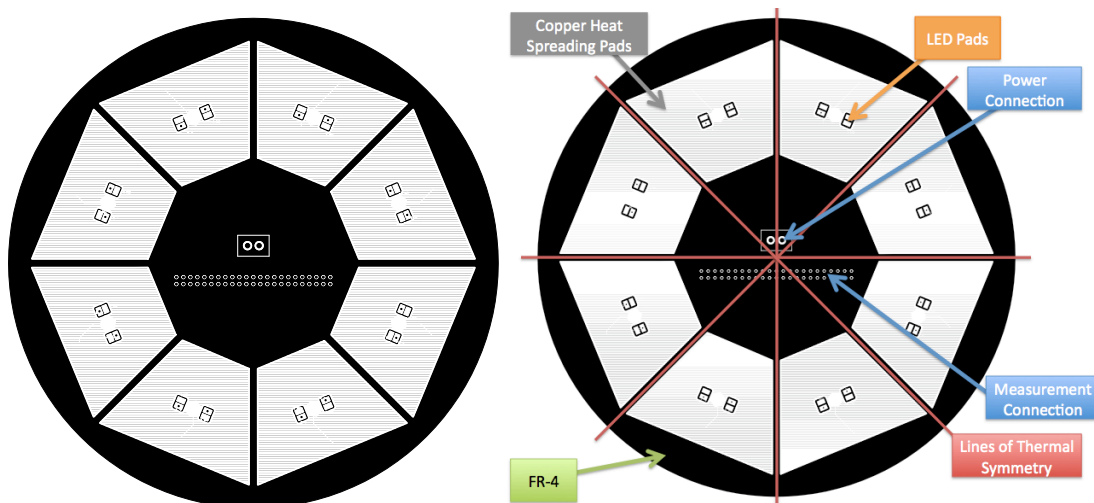
Figure 3.15: Image of PCB Vehicle and lines of thermal symmetry

These boards were modeled in SolidWorks and simulated in EFD.lab[4]. EFD.lab allowed for the analysis of the PCB layout using copper and FR-4[5] (a very common printed circuit board material), by simulating the shape of the LED chips. This was done to determine what the junction temperature of the LED would be before fabricating the PCB. This test

---

[4] EFD.lab was formerly known as FloEFD. This package was developed by Flomerics, which also developed FloTherm until Mentor Graphics bought them out. EFD stands for Engineering Fluid Dynamics

[5] FR-4 is made of woven fiberglass cloth with an epoxy resin binder that is flame resistant [20]. This material acts as an insulator between the layers of copper foil, which act as the traces for electrical connections.

showed that the FR-4 material would be able to sufficiently dissipate the heat. A concern

about FR-4's ability to act as a heat sink came up since FR-4 has very low thermal

conductivity, around 0.24 W/m-k. This is in contrast to aluminum, which ranges from

160-200 W/m-k and copper around 420 W/m-k. The simulation showed that by using

large copper fills there was sufficient heat spreading away from the LED despite the high

junction temperature. Figure 3.16 shows the thermal model of the circuit board being

tested. The test utilized lines of thermal symmetry to only solve 1/4th of the problem.

This saved computational time and resources.
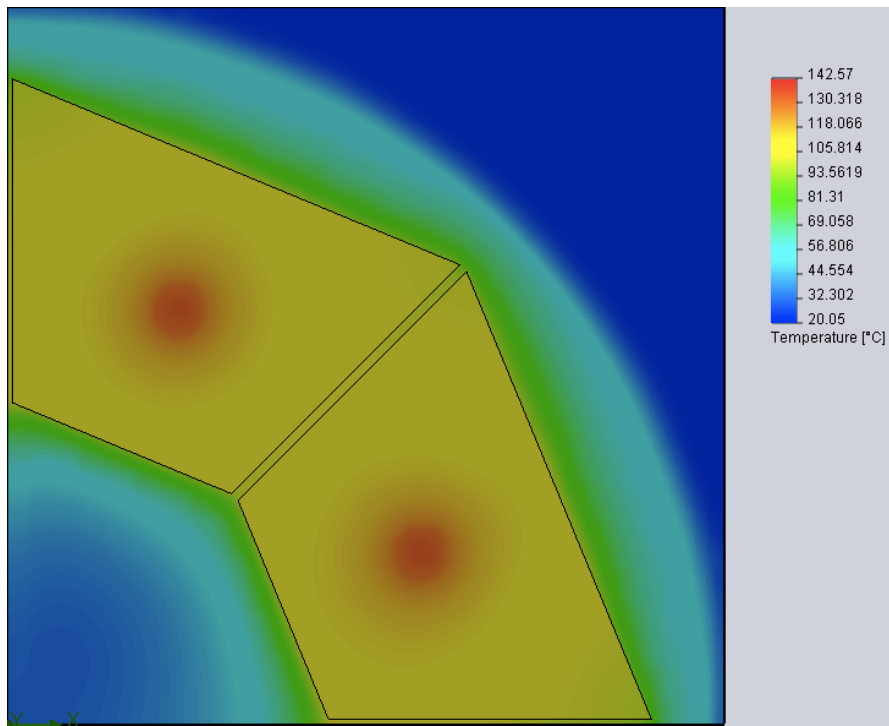
Figure 3.16: Thermal simulation of PCB test vehicle-using FloEFD.

After the thermal model, the boards were fabricated. After receiving the first

revision of the boards, it was determined that there was no connector that could

accommodate the pin layout that had been designed for the measurement connector. A

pin pitch (spacing) of 0.1" was selected, however it was required to be larger (0.167"

pitch) to accommodate a wire-to-board style connector that was needed. Otherwise a ribbon cable style connector was required which did not work with the wiring system that was previously designed. The system required twisted pairs and twisted pair ribbon cables were too expensive. It turned out to be cheaper to make a new PCB.
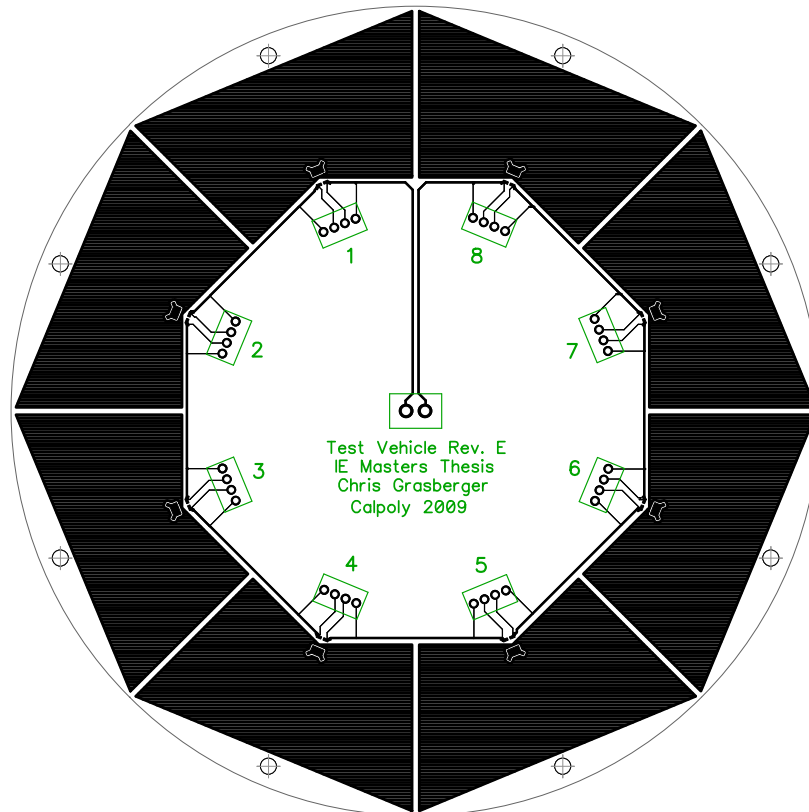
Figure 3.17: PCB Layout of the second revision of the test vehicle.

The new PCB design, shown in Figure 3.17, utilized a slightly different copper fill pattern and used common four position 0.1" headers with polarizing tabs to prevent incorrect wiring. While the shape is different than the first, it still utilized thermal symmetry. This model was not simulated in EFD.lab because the license had expired by the time this board layout was done. However, the board is very similar to the previous design and should net similar results.

The second revision of the boards was designed to follow the assembly and handling instructions of the manufacturer. On a side note, these boards were used to collect most of all of the data used in this thesis. Figure 3.18 shows the physical board compared to the datasheet. Only two small holes were removed due the extremely high cost of using a drill size that small. To use those holes would have made the boards cost nearly double the price. In an effort to save money, those holes were omitted. This change in the design would ultimately increase the thermal resistance of the design; however, measuring the thermal resistance and picking an aging current based on the measured value accounted for any change in the thermal resistance.
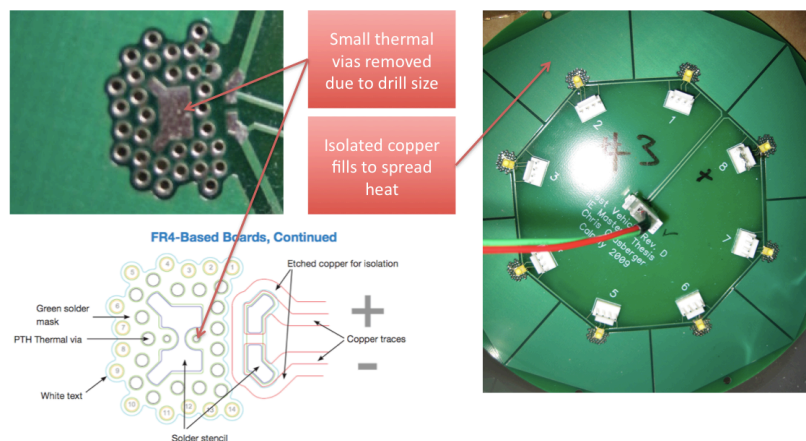
Figure 3.18: Image showing details of PCB Test Vehicle fabrication which matches recommended layout.

The LEDs selected were Philips LUXEON Rebel chips (LXML-PWM1-0070). Philips donated sixty of Rebel chips for the thesis. A close up of the chip is shown in Figure 3.19. These are high-powered chips; therefore, they are surface mount for improved thermal management.

Typically these chips are attached to PCBs via reflow soldering; however these LEDs were hand soldered. This was accomplished by heating up the wetting verification pads that were attached to the thermal pad that the LED sits on. See Figure 3.19 to see

the wetting pads on the PCB. After the pads were sufficiently warm and the solder had become a liquid, the LED was carefully placed on top of the hot solder with tweezers. After this solder had cooled, solder was then carefully applied to the wetting pads next to the anode and cathode connections. Once the solder had turned to liquid, capillary action took over and the solder moved under the LED. Shortly thereafter, the solder cooled and created a connection. This process was practiced on 15 chips, using the first revision of the PCB, before applying it to the second revision PCBs for actual testing.
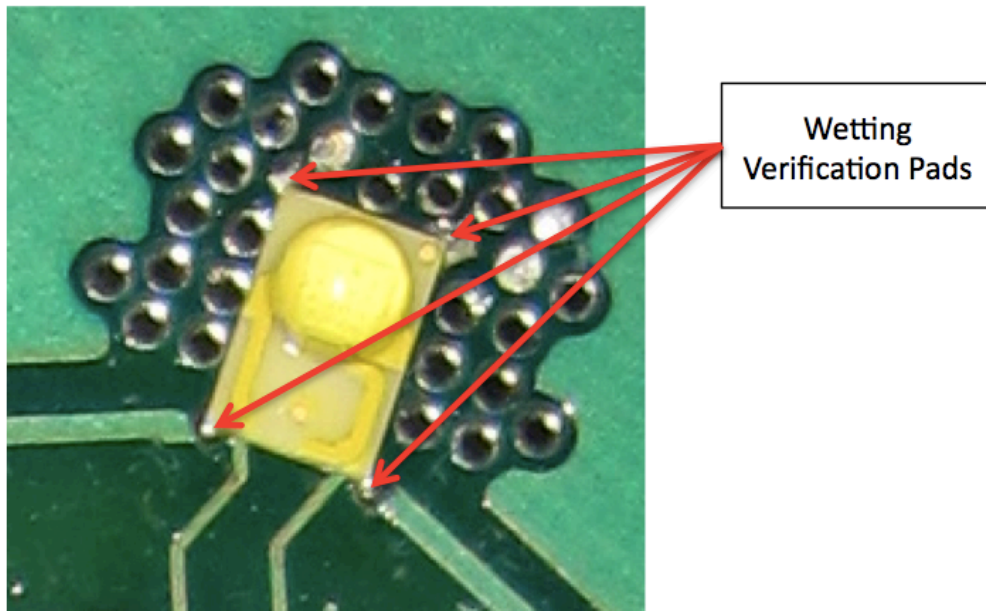
Figure 3.19: PCB wetting verification pads used for soldering.

There were concerns that this process damaged the LED, which may harm the results. Philips engineers said that the LEDs would exhibit damage, possibly in the form of current leakage, due to overheating from manual soldering. To verify this, the I-V curves of the data was plotted and compared with the datasheet. See the Data Analysis section for details on the results. However, the I-V curves were unknown at the time of the discussion with the Philip's engineers. They recommended using a reflow oven and also offered to assemble a new set of boards for this project. Having this opportunity,

there was a third revision of the PCBs fabricated using aluminum clad PCB (also known as Metal-Cored PCB – MCPCB). These boards also had thermocouples attached directly to the thermal pads for the option of collecting data using thermocouples. These boards were fabricated and some data was gathered from them. However, by the time these boards were ready for testing, it was nearing the end of the testing phase. As a result of this, little is known about the MCPCB circuit boards.

3.2.2 Testing Procedure

The design of the data acquisition system and the test vehicles were large parts of the project, however in the end, they were small stepping-stones before the actual thesis could begin. As described in previous sections, the PCB vehicle and data acquisitions system circuit boards were fabricated, assembled, and tested. After that point, the data collection started.

Each set of data combines information about voltage, current, and temperature to determine K-factors for an LED. The information includes five boards each with 8 LEDs, each LED at 3 currents (100, 350 and 700mA), and each current at 5 temperatures. Then there were five sets of data: Time 0, 1, 2, 3, and 4. These occurred at 0 hours, 405 hours, 1384 hours, 1980 hours and 3009 hours respectively. Ideally there were eight LEDs on each board, but due to LED failure and assembly errors, there were 37 in total between the 5 boards at time 0. One board with 6 working LEDs (the control), one board with 7 working LEDs, and the rest had 8 LEDs per board.

Collection of the data starts by placing all five boards into the oven. Once the LEDs had soaked in the oven for enough time to reach steady state, then the DAQ pulsed the LEDs at a specified current. This soak and pulse cycle (effectively a very low duty cycle) was done ten times to each LED, and the results were stored for averaging later. After those ten values were collected, the DAQ switched to the next LED and pulsed the new LED. This process was applied to all the LEDs on the board. Once complete, the current would then be changed. This cycle was continued until all LEDs on a board had been tested at all three currents.

After a board had been measured at the three currents on all the LEDs, the oven was opened, and the DAQ was wired to a new board. Since four-position headers were used, the process of wiring the 4-wire connections with the DAQ was quick. The oven was then allowed to soak again to return to its original temperature. Then this new board was subjected to all three currents on all of its LEDs and the data was stored. This process was repeated until all five boards had the data collected.

The oven was then set to be 20 degrees Celsius hotter than before. Once the LEDs had a chance to soak, data was collected on each of the five boards again. This process ended up being very slow in the end because rewiring the boards at higher temperatures took a great deal of time to allow the oven to reach its steady state temperature again. This process is depicted in Figure 3.20 and 3.21.

Data Processing

Calibration of LEDs in large industrial oven

Thermal Aging for 700+ Hours
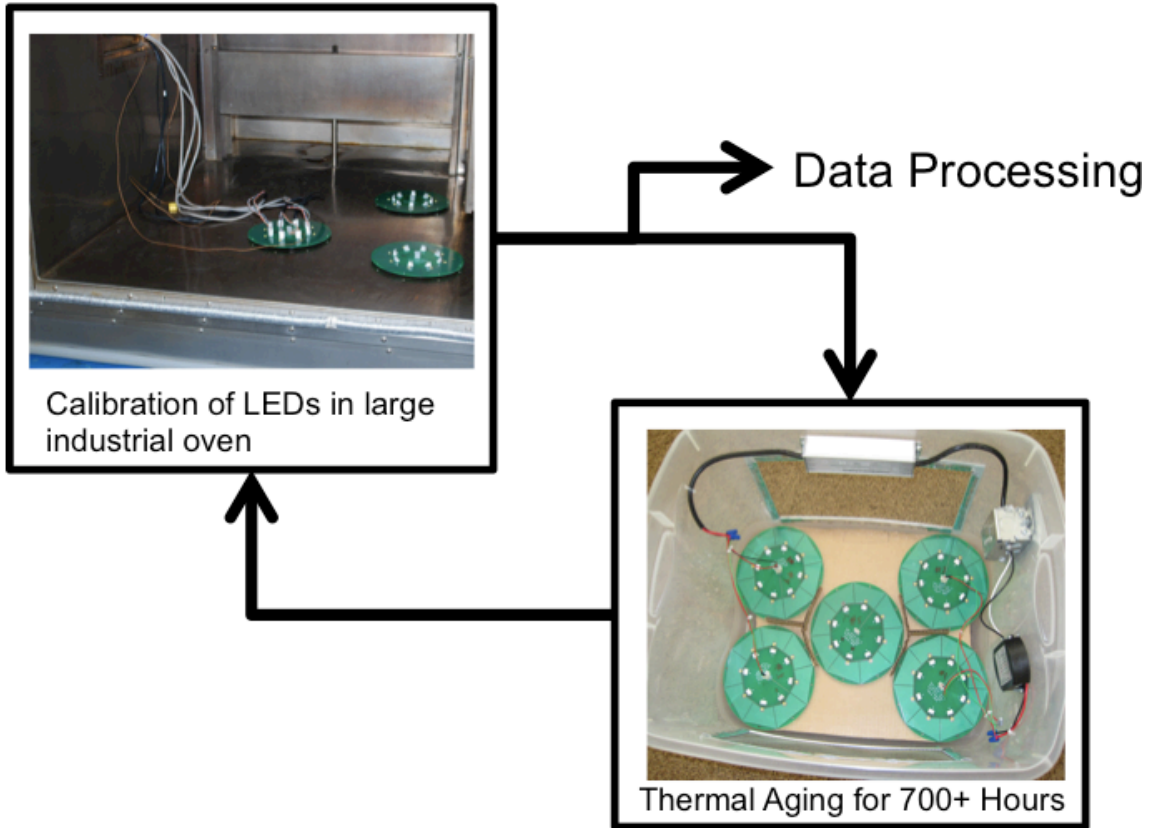
Figure 3.20: Collection Process Overview
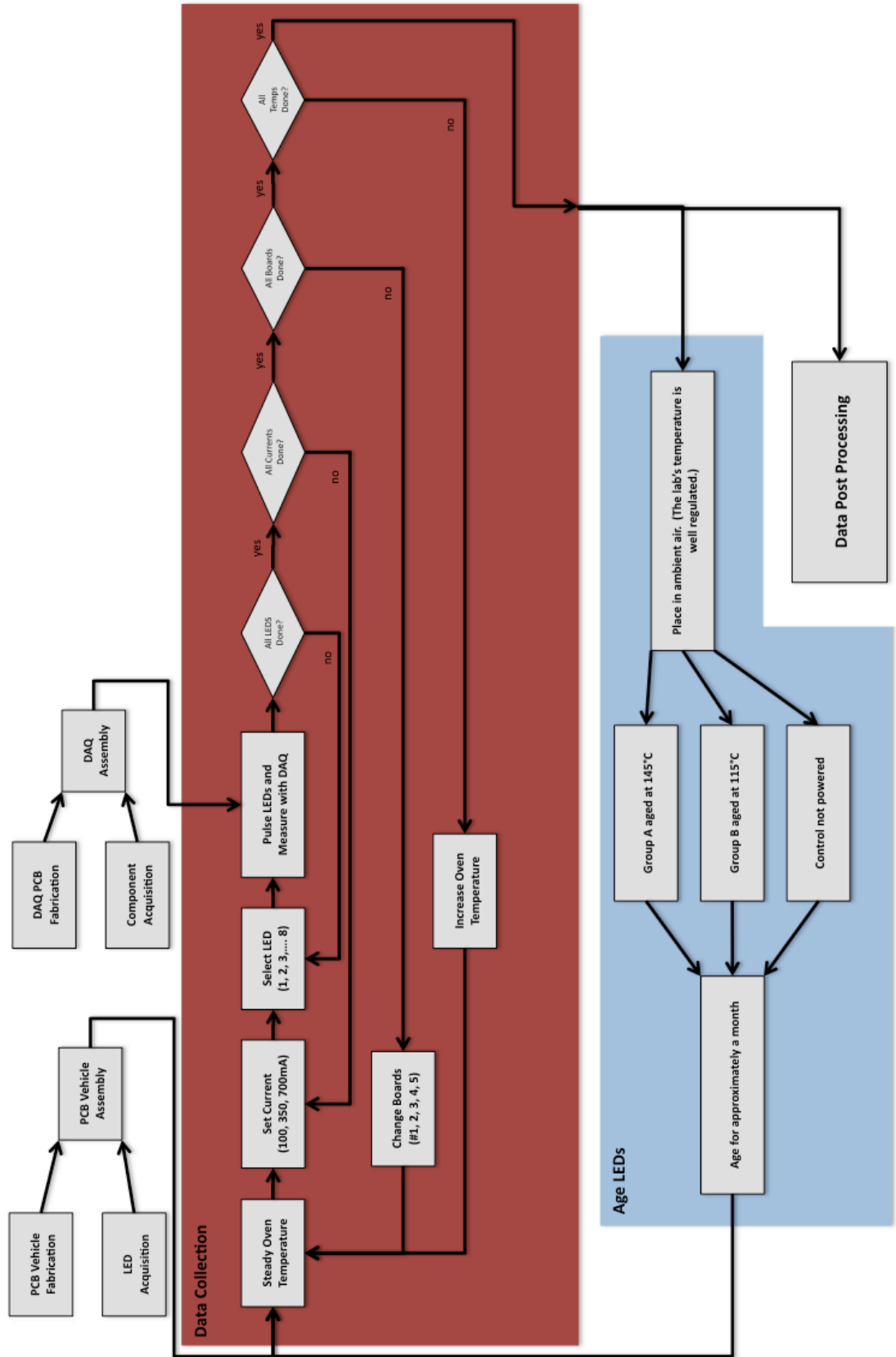
Figure 3.21: Flow chart to collect data

Step-By-Step Procedure

1. Place test vehicles in oven.
2. Connect first test vehicle to set of eight 4-position ramp headers. Each plug is numbered 1 through 8. If the board is missing chips or some have failed, connect using the lowest number plugs even if the numbers do not match. Example: If LED 2 is dead, then wire plug 1 to LED 1, plug 2 to LED 3, plug 3 to LED 4 and so on. This will leave plug number 8 disconnected at the end.
3. If the PCBs do not have an onboard thermocouple, there is loose probe within the wire bundle. Place the probe on top of the PCB to measure the air temperature near to LEDs. If the PCBs do have an onboard thermocouple, there is a K-type female connector in the wire bundle. Use this plug for onboard thermocouples.
4. Turn the oven on. There is a junction box to the right of the oven with a red lever. Turn the lever to the ON position.
5. Set desired temperature on the oven controller. The controller is on the side of the blue oven to the left of the junction box. Use the up and down arrows to select target temperature. With the exception of 20°C, set the oven about 4-8 degrees hotter than desired. The internal measurement is on the ceiling of the oven and there is a significant difference in temperature from top to bottom.
6. Connect the thermocouple plug to a hand held multimeter to read the K-type thermocouple. There are two male plugs next to the junction tester. One is an extension cable for onboard thermocouples, and the other is the male end of the probe inside the oven. Select which one you desire to measure
7. Turn on the computer. Username: droptest   Password: leadfree
8. Open LabView 8.6
9. Open latest version of Data Collection system. It should be version 5.
10. Turn on power supply (grey box) to the data acquisition system (blue box). Green power indicators, located on the blue box, should turn on.
11. Press the run in LabView just below the file menu. It is a triangle symbol similar to what would be found on a music player for play.
12. After a small loading delay, the LabView interface should begin to run. Two lights on the screen will illuminate. "Power" and "Boards" after both are green press the run button below them. If "Power" does not turn on, you need to check that you completed step 10. If "Boards" do not turn on, check that the two large cables coming from the computer are connected to the back of the blue the DAQ. If they are, check that they are connected to the right location.
13. Press the "All Off" button in the Resistor section and in the LED section. This will clear all past runs.
14. After both "All Off" sequences are done (the pull down menus for both will stop changing) select the 0.25Ω resistor in the pull down menu and press "Pulse Resistor." This will connect the 0.25Ω resistor as the current sensing resistor.
15. Press "Clear All" in the upper right area of the interface.
16. In the upper left corner, there is a teal region. There is a text field where 1-8 is entered. This is the number of LEDs to test on the test vehicle. If less than 8 chips are connected, ensure that the lowest plug numbers are used before the

higher plugs. If "7" is entered in this field, only plugs 1-7 are tested. After the value is entered, press the enter key to confirm the value.

17. To the right of this region there is a long green region. Within it, there is a section that is target current. Enter in the desired test current. Data collected has typically been 100mA, 350mA, 700mA for this thesis, however other chips may not be able to stand those currents. Accurate data can only be collected at 350mA and greater. The system can output a maximum of 1200mA. After the value is entered, press the enter key to confirm the value.

18. Further to the right is a target temperature area. Here is where you enter the oven temperature. This needs to be manually updated by the user by reading the handheld thermocouple reader that is connected to the probe near the PCB. Once the oven reaches steady state, it will not change too much. After the value is entered, press the enter key to confirm the value.

19. Press the "Process Board" button in the teal section. This will systematically measure all of the boards.

20. Press the "Save Bundle" button on the right side of the screen. This is the data collected during the "Process Board" sequence. After the file is saved, press the "Clear All" button.

21. After clearing the data from LabView, return to step 17. After all currents have been processed on the connected board, continue to the next step.

22. Open up the oven, and disconnect the test vehicle from the plugs. Then connect the plugs to the next test vehicle as done previously. Close the oven and wait for it to reach steady state temperature again. Then go to step 16.

23. After all of your test boards have been processed at the desired temperature, change the oven temperature to the next value. Wait until the temperature has reached steady state (about 20 minutes for 20°C increase) and go to step 16.

Chapter 4 - Data Analysis

An analysis of the data collected showed that the K-factor did change during aging. The data indicated that time was a statistically significant factor in the change in the K-factor. The change in K-factor was detected while there was no statistically significant change in the I-V curves; a change in the I-V curve might indicate degradation. Finally, the LEDs were damaged during assembly, which may have an adverse affect on these results.

Table 4.1: Summary of experimental design.

		Calibration Current		
		100mA	**350mA**	**700mA**
Aging Condition	**145°C** average junction temperature Group A Boards 1 and 2 (Aged with 470mA)	Data Rejected	Data Rejected	Data Rejected
	115°C average junction temperature Group B Boards 3 and 4 (Aged with 350mA)	Data Rejected	Analyzed	Analyzed
	Control Board 5	Data Rejected	Analyzed	Analyzed

4.1 100mA versus 350mA and 700mA Test Current Data

When the data acquisition system was designed, it was designed to be able to measure from 0.1mA up to 1000mA. However, with modifications to convert it from constant voltage to constant current, some stability issues arose. To resolve these problems, a resistor that was meant for testing at 1000mA was used for all current ranges. This is further discussed in section 2.1. By performing this modification, the ability to measure low currents was adversely affected. When a 100mA test pulse is measured across the 0.37Ω resistor, the measured voltage is 37mV. Compounding this problem, this signal is being measured 15 feet away, with a 30-foot length of cable. While the signal is transmitted through a twisted pair to reduce noise, noise still gets into the signal. The amount of noise in the signal compared to the signal itself becomes noticeable. This caused the results of 100mA measurements to be highly unpredictable. Figure 4.1 shows a plot of the K-factor versus time for the control board. Linear trend lines were applied to all three data series to show their linearity. The data at 700mA and 350mA shows that they agree fairly well with the trend line. The trend line is nearly horizontal as it is expected to be for a board that has never been stressed with any aging. This is in comparison to the 100mA data, which does not agree with a linear trend line. The 100mA data should be flat and linear as in the 350mA and 700mA data sets. Both Group A and B also exhibit this trend of the data being erratic at 100mA.
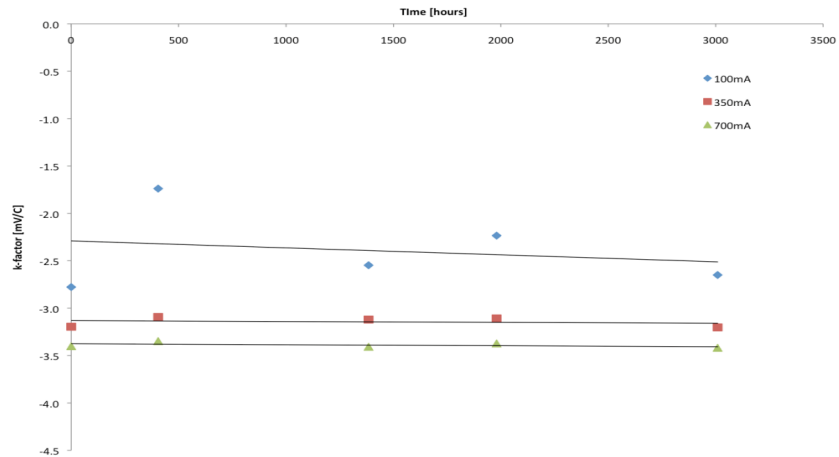
Figure 4.1: Average K-factor values versus time. 350 and 700mA data follows a linear trend line as expected, however 100mA data is erratic indicating errors at low current measurements.

Using Minitab, the results from K-factor values at different current levels were compared versus time. Initially, the data was assumed to be normal and a One-Way ANOVA analysis was performed on each test current level (100, 350, and 700mA) and was compared versus time. For an ANOVA analysis the following two hypotheses are used:

H_0: All means are the same

H_A: At least one mean is not the same

The results indicated that the 100mA test current was highly dependant on time with a P-value of 0.000. The 350mA and 700mA test currents were independent from time with P-values greater than 0.9. The board being studied was the control; none of the test currents should be dependant on time.

Unfortunately, the residual plots from the analysis indicated that the data was not normal. Figure 4.2 shows the residual plots for 100mA, 350mA, and 700mA test currents versus time. ANOVA is relatively robust against lack of normality, however a non-parametric study was conducted to verify the results of the ANOVA analyses.
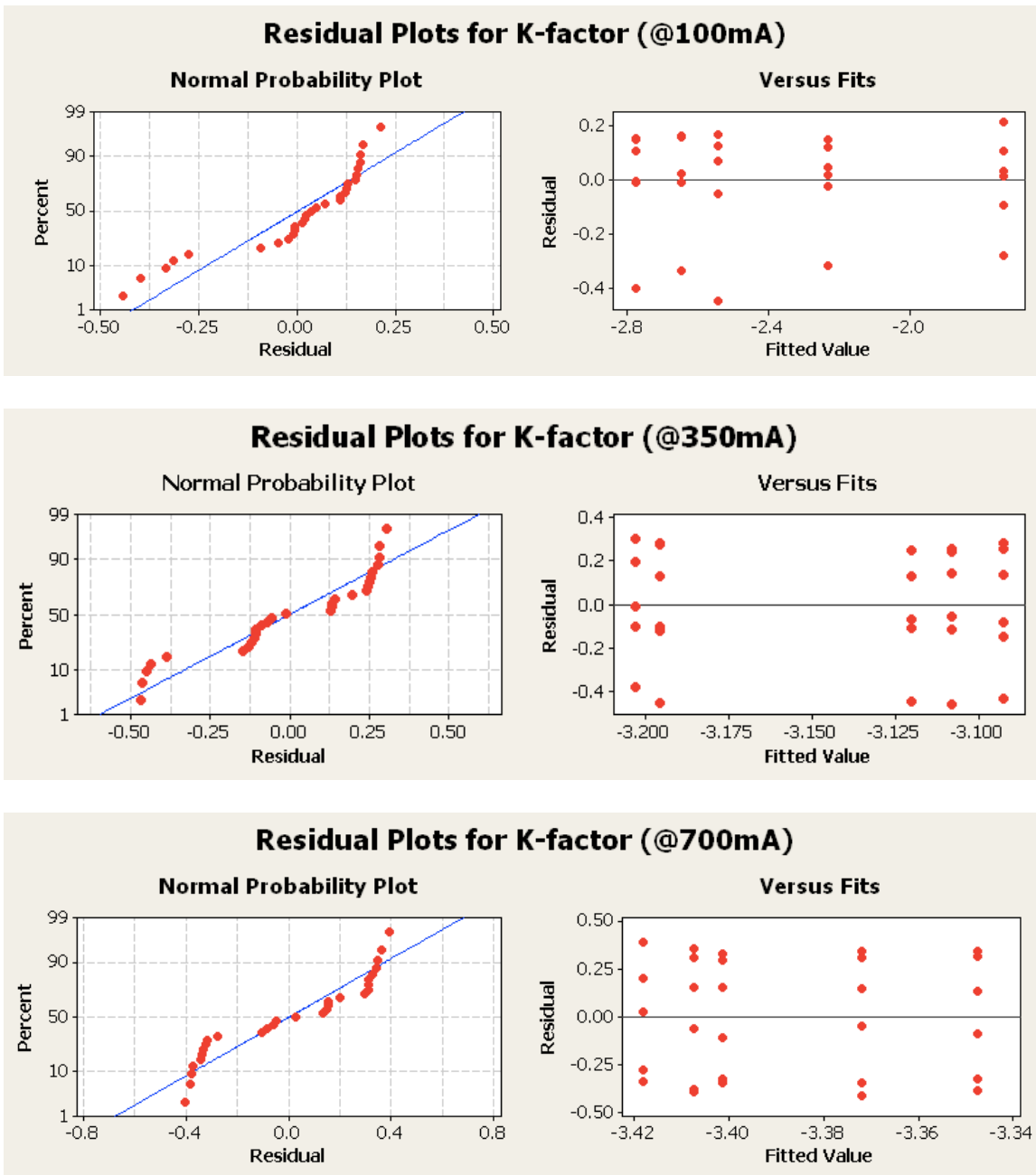
Figure 4.2: Normality and Residual versus Fitted value plots for K-factor versus Time at 100mA, 350mA, and 700mA. P-value <0.005 for the normality test in each case indicating a lack of normality.

A Kruskal-Wallis non-parametric test was performed on the data. The hypothesis for this test is different from that of an ANOVA test, which checks if all means are the same. The Kruskal-Wallis test uses the median. The following hypotheses are used for the test:

H_0: **Medians are equal**

H_A: **Medians are not equal**

Table 4.2 shows the result for this test for each test current level. At 100mA, a P-value of 0.000 was determined. Therefore, the null hypothesis should be rejected which means that the medians are different. When testing 350mA, a P-value of 0.743 is calculated. Such a high P-value indicates that the test fails to reject the null hypothesis, which would indicate no significant difference in the medians. A similar result with 700mA, a P-value of 0.921 was calculated.

The initial One-Way ANOVA analysis of each current level may have been invalid due to lack of normality, however the results from that initial study matched that of the non-parametric study, which does not require normal data. Since the control board had never been aged, there should be no change at any current level. The results from the analyses and plots for 350mA and 700mA test currents agree that there was no change due to time on the control board, as expected. However, at 100mA there was a statistically significant change when there should not be. As a result of this, the 100mA test current data was rejected on all 5 boards.

Table 4.2: Kruskal-Wallis Test for K-factor versus Time for the control board. The 100mA test current shows that time is significant, however the 350mA and 700mA test currents show that time is not significant.

```
Kruskal-Wallis Test: K-factor (@100mA) versus Time
Time
(@100mA)   N  Median  Ave Rank      Z
   0.00    6  -2.726       5.7  -3.01
 404.75    6  -1.714      26.5   3.71
1384.25    6  -2.450      13.2  -0.59
1980.25    6  -2.202      19.5   1.45
3009.00    5  -2.627       9.2  -1.67
Overall   29              15.0

H = 22.43  DF = 4  P = 0.000


Kruskal-Wallis Test: K-factor (@350mA) versus Time
Time
(@350mA)   N  Median  Ave Rank      Z
   0.00    6  -3.183      12.3  -0.86
 404.75    6  -3.070      17.5   0.81
1384.25    6  -3.089      15.7   0.22
1980.25    6  -3.066      16.8   0.59
3009.00    5  -3.214      12.2  -0.81
Overall   29              15.0

H = 1.96  DF = 4  P = 0.743


Kruskal-Wallis Test: K-factor (@700mA) versus Time
Time
(@700mA)   N  Median  Ave Rank      Z
   0.00    6  -3.380      14.0  -0.32
 404.75    6  -3.324      17.3   0.75
1384.25    6  -3.361      13.0  -0.65
1980.25    6  -3.324      15.8   0.27
3009.00    5  -3.394      14.8  -0.06
Overall   29              15.0

H = 0.92  DF = 4  P − 0.921
```

4.2 K-factor of LEDs aged at 145°C (Group A)

The choice to use two aging temperatures was driven by the need to ensure that data was possible to collect after the duration of accelerated aging. Group A was aged with an average junction temperature of 145°C (using 470mA during aging) and Group B was aged at 115 °C (using 350mA during aging). While the datasheet quoted a maximum junction temperature of 150 °C, there is reason to believe that a few of the chips still were beyond that temperature.

Group A began to fail very rapidly after 405 hours (approximately 17 days) and 25% of Group A's LEDs had failed. At 1385 hours (~58 days) all of the LEDs in Group A had failed. While this had always been a possibility, very little data was collected on these LEDs. As a result, only two data points were measured. Time 0, and Time 1 at 405 hours. It is nearly impossible to gather useful trend data from two data points while knowing that the measurements can vary from time period to time period. Figures 4.3 and 4.4 show the K-factor versus time for board 1 and board 2 respectively. These two boards together make up Group A (145 °C).

The sheer lack of data makes it difficult to compare results and have confidence in the data. Due to the lack of data for Group A, the results will not be considered in the determination of the K-factor's degradation.
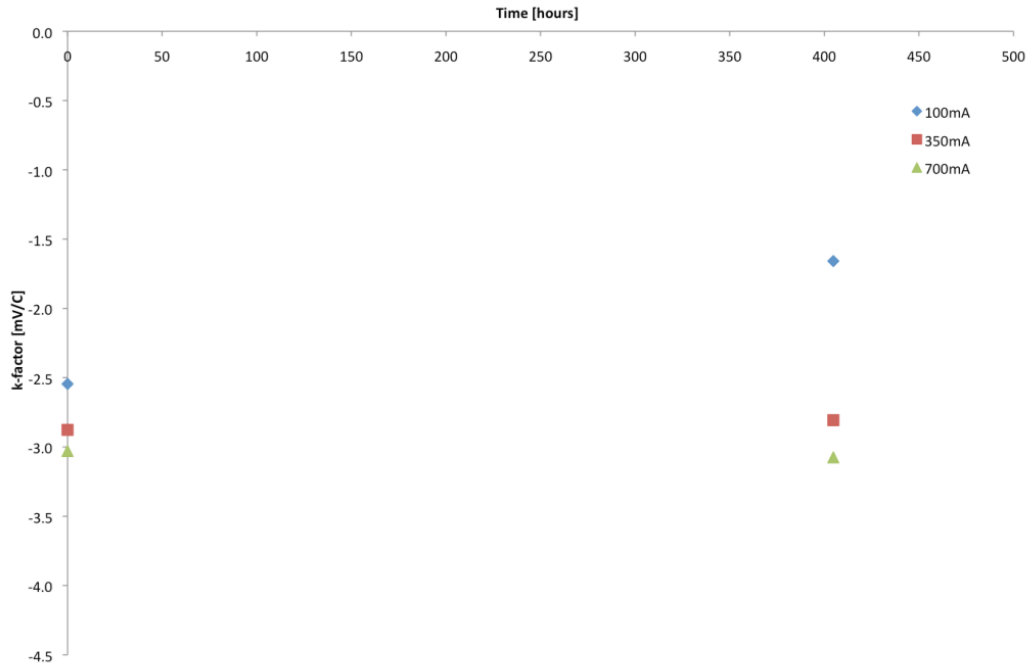
Figure 4.3: Board 1 K-factor versus time.
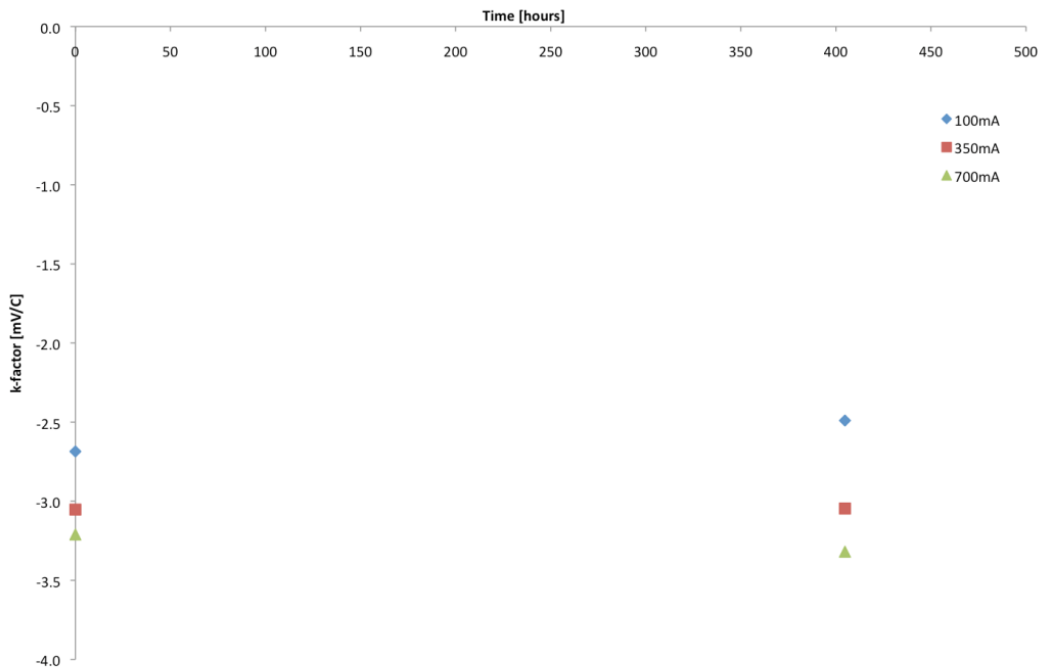
Figure 4.4: Board 2 K-factor versus time.

4.3 K-Factor Changes for Data Aged at 115°C (Group B)

The heart of this research is the forward-voltage to junction-temperature coefficient, K-factor, degradation. Despite many setbacks and challenges in verifying data occurred, it does appear that there is a significant effect of time on the K-factor's degradation. While the testing period is too short to determine a model to predict future degradation, there is indeed a statistically different value in the K-factor.

Results in section 4.1 showed that the data collected at 100mA was rejected due to erratic values, most likely due to measuring at the limits of the DAQ's capabilities. Results in section 4.2 show that Group A, which was aged at 145°C, degraded too rapidly to collect useful data. Due to rapid failure of Group A, only Group B's (aged at 115 °C) data is used in the analysis of K-factor degradation as presented in section 4.2.

With all of the factors considered in this study, there appears to be a significant change in the means of the K-factor with respect to time. Table 4.3 shows a Minitab General Linear Model analysis of the K-factor versus the boards, time, and test current. While the study is interested purely in the change due to time, the boards within Group B (board 3 and board 4) appear to be significant in this study. The boards have a P-value of 0.033, which indicates that the null hypothesis is rejected (H_0: $\mu_{B3} = \mu_{B4}$; H_A: $\mu_{B3} \neq \mu_{B4}$). In other words, the two boards in Group B were not the same on average. Also, the study shows that the test current is significant. This is expected, as shown in Equation 2.2, that the K-factor is dependant on the test current.

The final, and most important, factor is the time. The time is also a highly significant factor in the analysis. The low P-value of 0.000 indicates that the null hypothesis should be rejected. This means that at least one of the time intervals average

is different than another.   Analyzing the data at each of the time intervals reveals that the

initial calibration is significantly different than time period 2, 3, and 4.   This can also be

seen in the main effects plot shown in Figure 4.5. The results showed that from the initial

calibration to the third calibration that there was a 10.4% change in the K-factor.

The main effects plot, Figure 4.5, showed that both current and board factors are

important. However, the time is also critical. Interestingly enough the values increase

and then dips at the end. This dip at the end occurs for an unknown reason at this time.

Table 4.3: Minitab analysis of K-factor versus board, time, and current.

```
General Linear Model: K-factor versus Time, Board, Test Current
Factor         Type    Levels  Values
Time           fixed        5  0.00, 404.75, 1384.25, 1980.25, 3009.00
Board          fixed        2  3, 4
Test Current   fixed        2  0.35, 0.70


Analysis of Variance for K-factor, using Adjusted SS for Tests


Source          DF    Seq SS   Adj SS   Adj MS       F       P
Time             4    2.4951   2.6737   0.6684    6.51   0.000
Board            1    0.4769   0.4769   0.4769    4.65   0.033
Test Current     1    1.5010   1.5010   1.5010   14.62   0.000
Error          121   12.4222  12.4222   0.1027
Total          127   16.8952
```
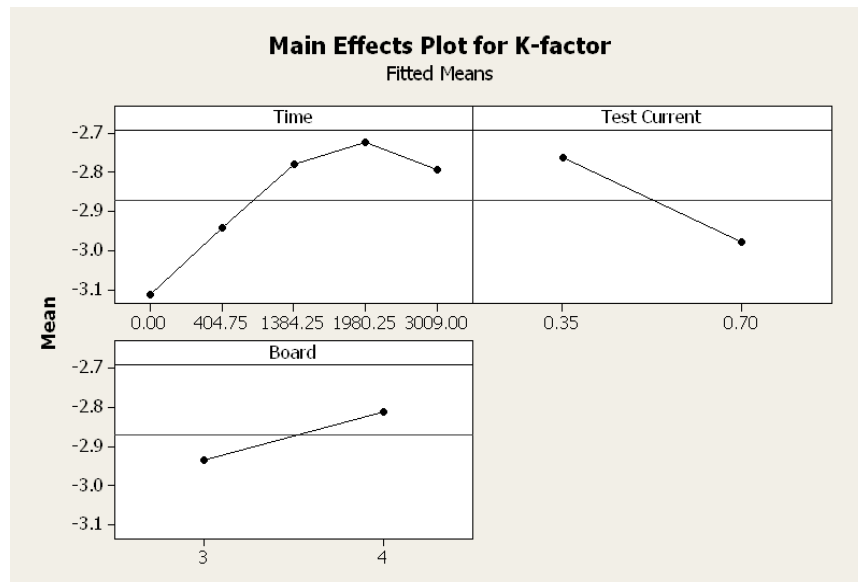

Figure 4.5: Main effects plot for K-factor versus Board, Time (Hours), Current

Finally, the residual plot was analyzed. Figure 4.6 shows the residual plot. When testing the residuals manually, a P-value of 0.131 is calculated. This indicates that the data is normally distributed. The plot of residuals versus fitted value appears to be reasonably random enough to satisfy the constant variance requirement. Finally, looking at the residual versus observation, there appears to be some data that has a fairly large residual at the midpoint and at the end. The data was entered in as board 3 from time 0 to time 4 and then board 4 from time 0 to 4. So the middle point and end point that shows a lot of residual in fact is from time 4. At this time, the reason for this large residual is unknown.
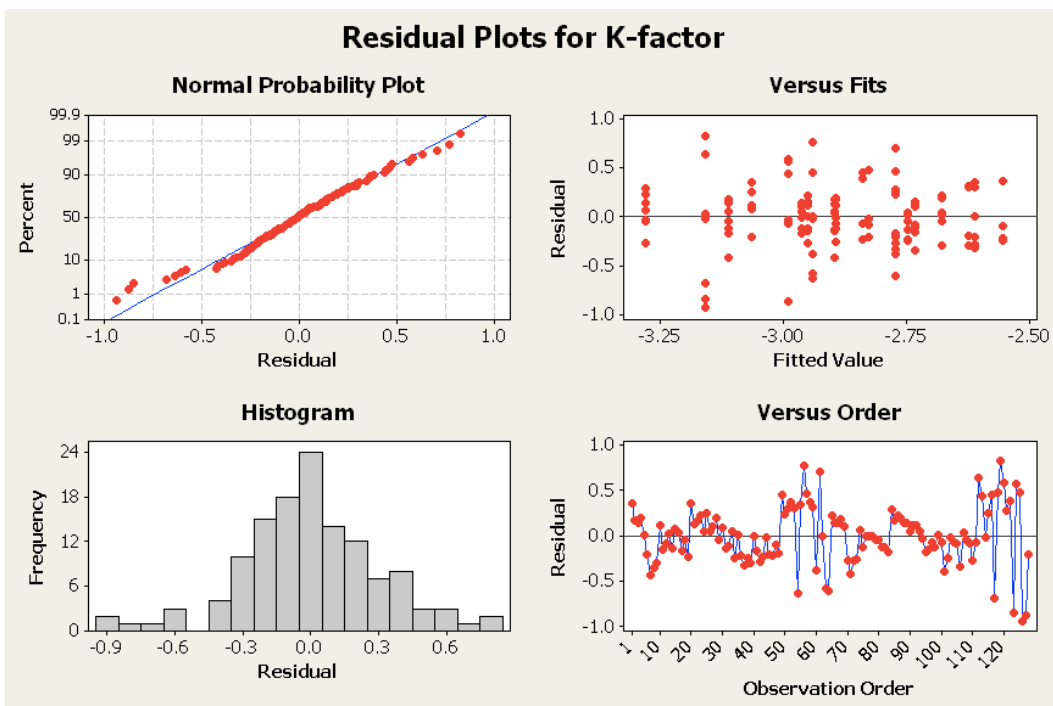
Figure 4.6: Residual plot for analysis of K-factor versus Board, Time, Current. The normality test has a P-value of 0.131, which indicates normal data.

4.4 Characteristics of I-V curves

4.4.1 Initial I-V Curve Characteristics

There were concerns that hand soldering the LEDs would cause damage to the chips. Engineers at Philips LumiLEDs recommended checking the I-V curve against the datasheet for LUXEON Rebel chips. At first the data appeared to show that the LEDs were not damaged as the Philips engineers suggested. However, upon comparing to data collected from the boards assembled by Philips and the boards that were hand soldered, there was a distinct difference in the I-V curves, which might indicate damaged LEDs. The LEDs did show above average forward voltages, which according to the datasheet and engineers is a sign of a damaged or degraded LED.

The methodology that Philips uses to measure their I-V curve is not entirely reproducible with this experiment. Their method requires taking a LED and applying a set current. While the LED is operating, they used an environmental chamber where they regulated the ambient temperature so that the LED's thermal pad temperature was always 25 °C throughout the experiment. Using this approach, they generated the I-V curve for their LEDs. Additionally, Philips grouped Cool-white, neutral-white, warm-white, green, cyan, blue, and royal blue LEDs together to generate the I-V curve.

This approach to generating I-V curves is not reproducible with the collected data for this experiment. It is not feasible due to the time it would take to reach a steady state temperature of 25 °C for 37 LEDs, one at a time and then do this at all five measurement time periods. It becomes especially difficult since I-V plots were not analyzed until after the second of set of data was collected. This problem was resolved by using the

knowledge about each LED's K-factor and voltage offset. Figure 4.7 shows a typical K-factor plot developed from collected data.

V = -0.0031T + 3.5673
R² = 0.99733

V = -0.0029T + 3.3423
R² = 0.99678

V = -0.0025T + 3.0462
R² = 0.99577
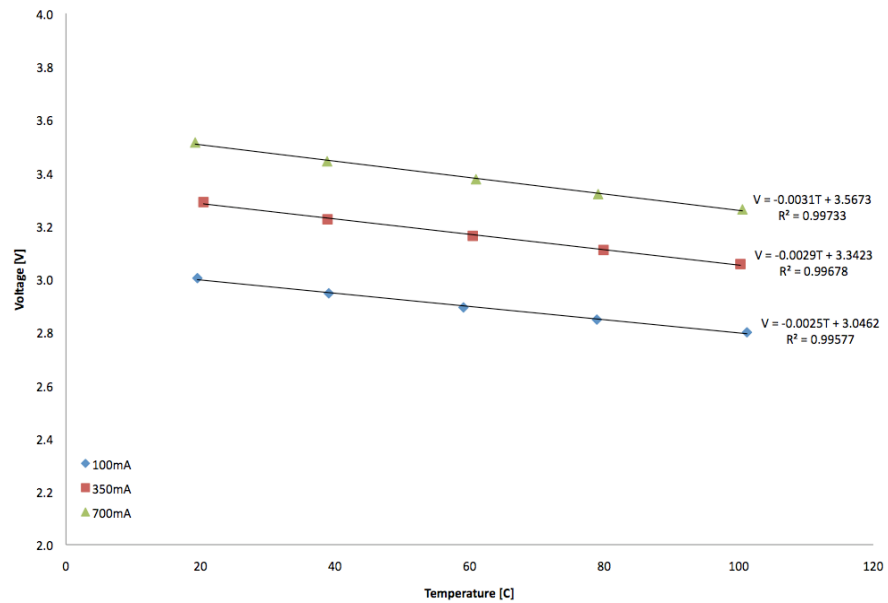
Figure 4.7: Typical K-factor plot generated from collected data.

Using the measured values from each LED, I-V curves were calculated for a junction temperature of 25°C. This differs from how Philips measures the results by using a thermocouple attached to the base of the LED's thermal pad. The recommended test location is shown in Figure 4.8.

Recommended test point
for a thermocouple
(on the wetting verification pad)
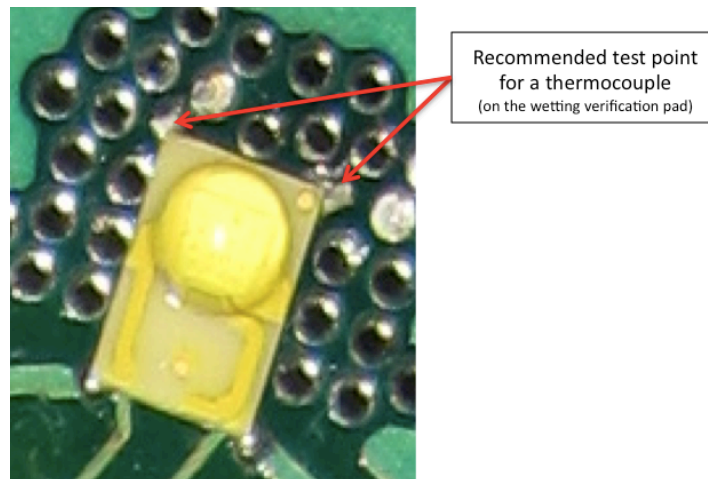
Figure 4.8: Recommended test location using thermocouples.

By using the thermal resistance of the package to estimate the forward voltage, Equation 4.1 can be developed. This equation determines the forward voltage at a specified thermal pad temperature, $T_{thermalpad}$, instead of the junction temperature. The forward voltage of the junction temperature is what was collected in this thesis, which is why Equation 4.1 was needed to convert the data to compare with Philip's results.

Equation 4.1: Equation to determine the forward voltage of the LED junction if the thermal pad temperature is specified instead of the junction.

Using Equation 4.1, plots of the I-V curves were made and then compared to the datasheet. Figure 4.9 shows typical board assembled by Philips using reflow soldering to attach the LED packages to a metal-cored PCB. Figure 4.10 shows a typical board that was assembled by hand with a soldering iron. The boards that were assembled with a soldering iron have a distinct shift to the right in the I-V curves for all of the LEDs on the board. This would indicate that there was damage to the LED, which has resulted in an increased the nominal voltage for these diodes. This is in contrast to the boards that were assembled using a reflow oven. Most of the LEDs in Figure 4.9 fall nearly on top of the datasheet's line with the exception of an outlier. Both of these cases are typical for their assembly methods based on the boards that were used to collected data. The board shown in Figure 4.10 is the control test for the data in this thesis.

Between figures 4.9 and 4.10, there is a distinct difference in the I-V curves. This indicates that hand soldered LEDs were damaged during assembly. This would also indicate that the reflowed boards should be used for data collection instead of the hand-soldered LEDs. Unfortunately, too little information is known about the reflowed boards

due to the time it took to fabricate them. Therefore, the hand-soldered boards are used

for the analysis of this topic since adequate data is available on these boards.
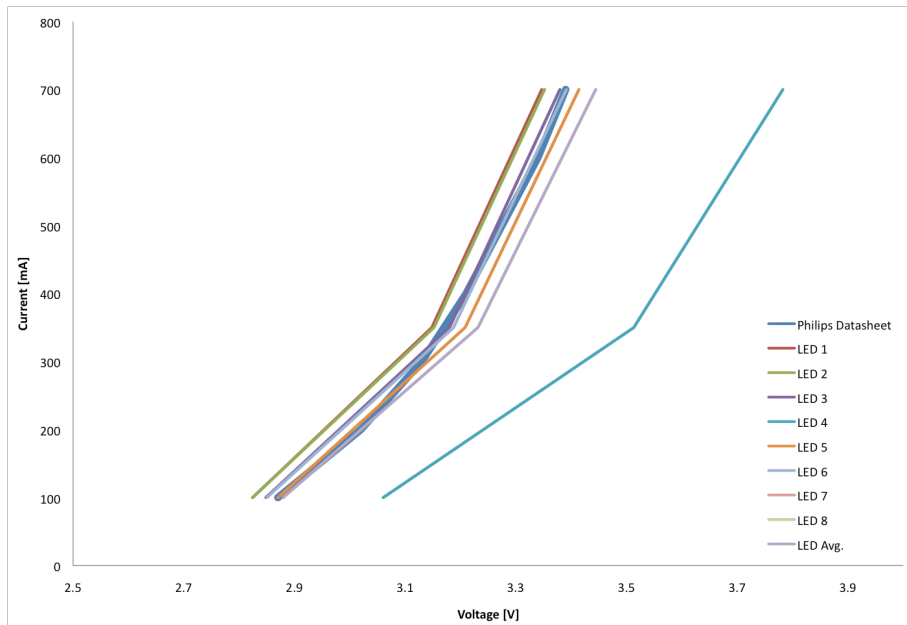
Figure 4.9: Typical plot of LED I-V curves, at timer zero, for metal-cored PCB using reflow soldering compared to Philips Datasheet.

Note: Curve to the far right (LED 4) is not the datasheet curve but rather an outlier.
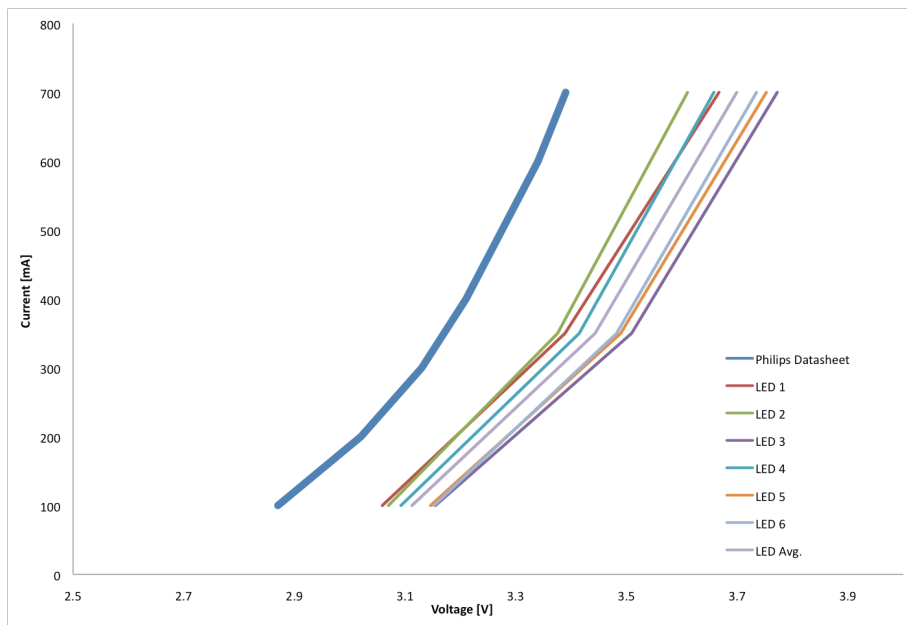
Figure 4.10: Typical plot of LED I-V curves, at time zero, for FR-4 PCB using hand soldering compared to Philips Datasheet.

4.4.2 Changes in I-V Characteristics due to Aging

A critical component of this test was the ability to accelerate testing. Since LEDs can last for over 50,000 hours given the right conditions, it was critical that the tests be accelerated so that results could be seen sooner. The primary objective of having two groups, at different temperatures, was to ensure that there were results due to degradation in at least one of the two groups. As mentioned in section 4.2, Group A (aged at 145°C) failed very rapidly due to high junction temperatures. For this study, Group A was the extreme for too much degradation and the control was the case of no degradation. However, the amount of degradation to Group B (aged at 115°C) needed to be determined.
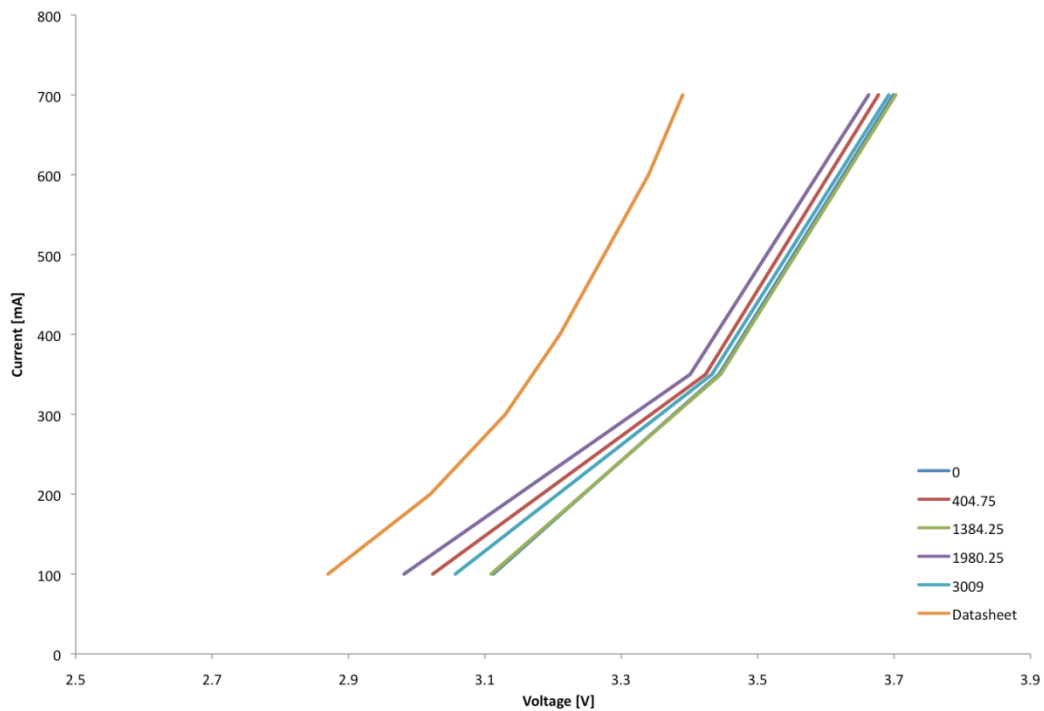
Figure 4.11: I-V curve of control board average values. These curves are from different test points and compared to the datasheet.

The control board, board 5, was never aged. This would imply that the I-V curves should not show a shift in value. Figure 4.11 shows a plot of the control board average I-V curve at each test period compared to the datasheet. As mentioned in section 4.4.1, there was a shift to the right from the datasheet due to degradation caused during assembly. However, there was varying I-V curves at different times and it is necessary to determine the significance of this. Initially an ANOVA test was performed with forward voltage (V_f) versus current and time. However, the data proved to be not normally distributed. Figure 4.12 shows the residual plot from the initial ANOVA test.

Since the data was not normal, the Kruskal-Wallis non-parametric test was used. The two hypotheses for the Kruskal-Wallis test are:

H_0: Medians are equal

H_A: Medians are not equal

Table 4.4 shows the results of the test of V_f versus time. The study was also broken up into the two different current levels as done in section 4.3.1. In the 350mA test current data, a P-value of 0.422 calculated, which indicates that the test fails to reject the null hypotheses and therefore there is not a significant difference in the median value at all time periods for the control board. Similar to the test current data at 350mA, 700mA also failed to reject the null hypotheses with a P-value of 0.644. This result was expected since the control board should have nearly identical I-V curves since it was never aged.
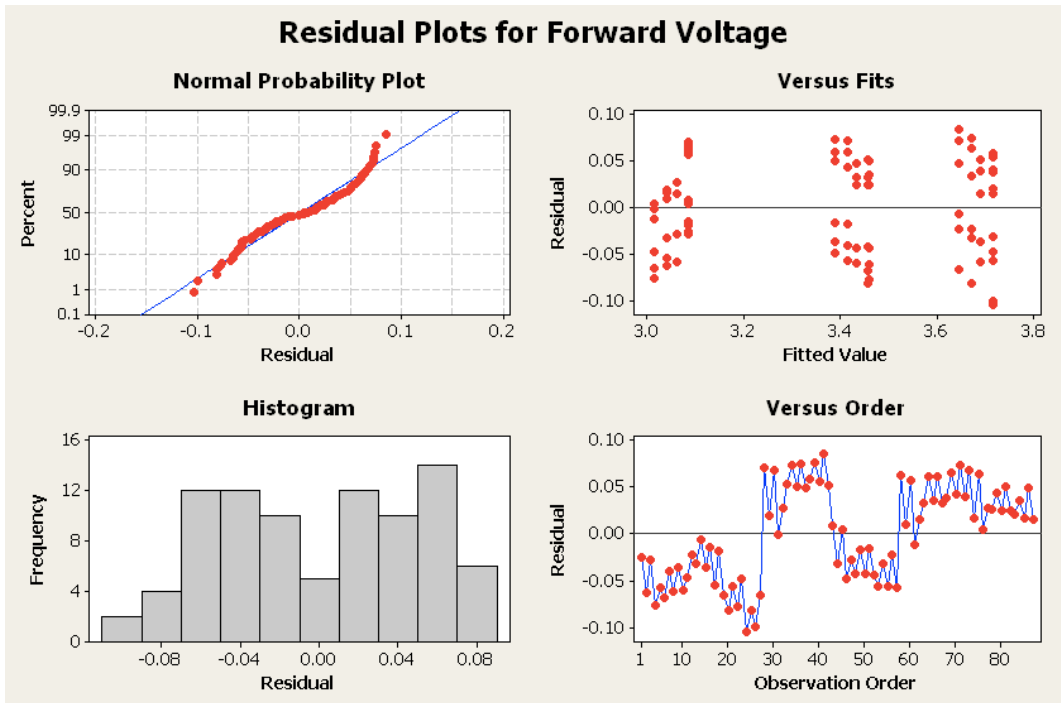
Figure 4.12: Residual plots of an ANOVA analysis of the control board showing the data is not normally distributed. P value for normality test was <0.005.

Table 4.4: Analysis of the significance of the control's I-V curves vs. time. The analysis is broken up into two different test current levels, 350mA and 700mA.

```
Kruskal-Wallis Test: Vf (@350mA) versus Time (@350mA)
Time
(@350mA)   N   Median   Ave Rank      Z
   0.00    6    3.448      20.2     0.89
 404.75    7    3.424      16.0    -0.31
1384.25    7    3.446      20.6     1.10
1980.25    7    3.401      11.6    -1.67
3009.00    6    3.445      17.2     0.05
Overall   33               17.0


H = 3.88  DF = 4  P = 0.422



Kruskal-Wallis Test: Vf (@700mA) versus Time (@700mA)
Time
(@700mA)   N   Median   Ave Rank      Z
   0.00    6    3.701      19.5     0.70
 404.75    7    3.677      15.9    -0.35
1384.25    7    3.702      19.9     0.88
1980.25    7    3.663      12.7    -1.32
3009.00    6    3.699      17.5     0.14
Overall   33               17.0


H = 2.50  DF = 4  P = 0.644
```

In stark contrast to the control is Group A, which was aged at 145°C. This group failed due to degradation after the second testing period. If these LEDs had not run at a junction temperature of 145°C as long, the degradation would have been less and the LEDs would have not failed. Therefore, the amount of degradation should be strongly dependant on time. Similar to the Control board, an ANOVA test was first done. The resulting residuals were indeed normally distributed. Figure 4.13 shows the result of this test. However to keep the test type the same, a Kruskal-Wallis test was performed. It should be noted that the results from the ANOVA test and Kruskal-Wallis test yielded the same results.
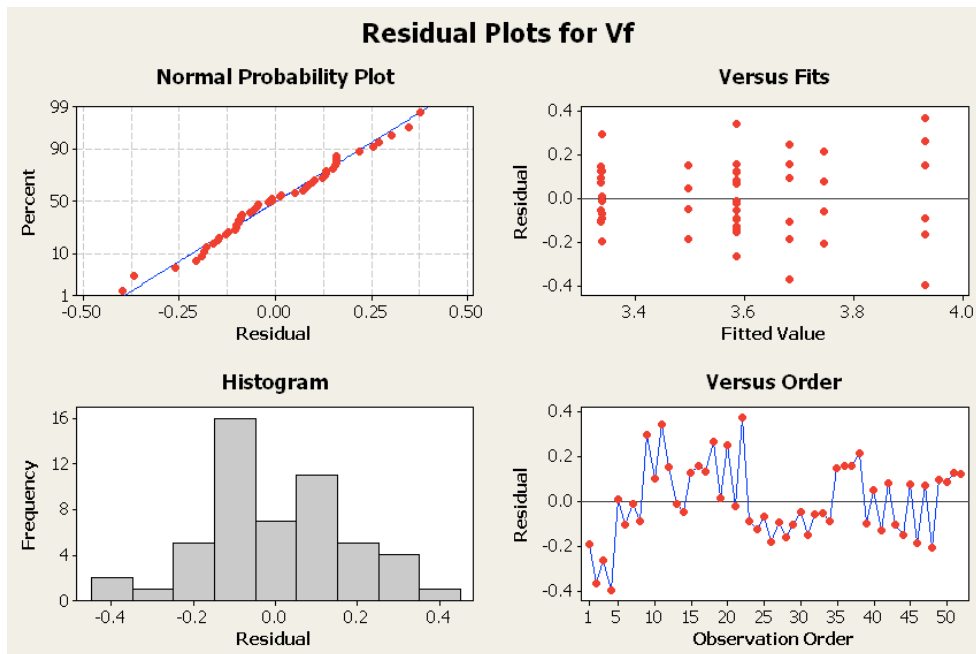
Figure 4.13: Residual plots for Group A (aged at 145°C) from an ANOVA analysis. The data appears to be normally distributed with a P value of 0.462.

Figure 4.14 shows Group A's two I-V curves against the datasheet. Since there are only two curves, it is easy to see that there is a shift to the right. However, the plot does not show if this is statistically significant. Table 4.5 shows the Kruskal-Wallis test and the resulting P-value of 0.001 for 350mA test current and 0.003 for 700mA. In both

cases the null hypothesis was rejected. Therefore there was a statistically significant change in the medians before the LEDs failed. This was expected as it is clear that time at a high current, which resulted in a high temperature, caused rapid failure. It should be noted that any LED that was outside the bounds of the datasheet's nominal value at 350mA was considered failed. This means a voltage less than 2.55V or greater than 3.99V at 350mA was considered to be failed. However, the LEDs in Group A were all below 1V, most were below 0.1V.
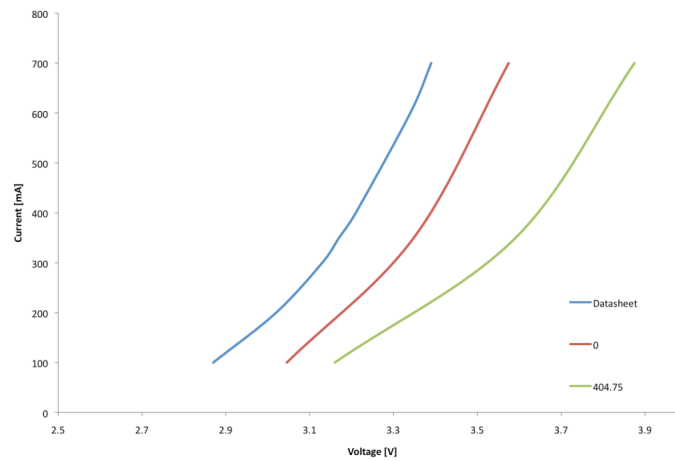
Figure 4.14: Plot of the Average I-V curves for Group A at different times.

Table 4.5: Minitab analysis of Group A's I-V versus time. The results are separated into 350mA and 700mA test currents.

```
Kruskal-Wallis Test: Vf (@350mA) versus Time (@350mA)
Time
(@350mA)    N    Median   Ave Rank      Z
  0.00      17    3.348      10.6     -3.28
404.75      12    3.562      21.2      3.28
Overall     29               15.0

H = 10.74   DF = 1   P = 0.001


Kruskal-Wallis Test: Vf (@700mA) versus Time (@700mA)
Time
(@700mA)    N    Median   Ave Rank      Z
  0.00      16    3.551      10.0     -2.95
404.75      10    3.834      19.1      2.95
Overall     26               13.5

H = 8.71   DF = 1   P = 0.003
```

Figure 4.15 shows a plot of Group B's I-V curves at different times. Looking closely at the curves, the value appears to shift left then to the right. The plot appears to be much like that of the control test; however it is hard to be certain. The data for this Board's I-V curves was not normally distributed. Figure 4.16 shows the residual plot for the initial ANOVA test. A non-parametric test was then done which is shown in Table 4.5. These results are somewhat inconclusive. At 350mA, the P-value was 0.072. At a 5% level of significance, the null hypothesis fails to be rejected. At 7.2% or higher, it is rejected. However, at 700mA, the P-value was 0.399, which indicates that the test fails to reject the null hypothesis. The initial ANOVA study determined a P-value of 0.316. These results indicate that there was most likely not a significant change in the I-V curves due to time in Group B.
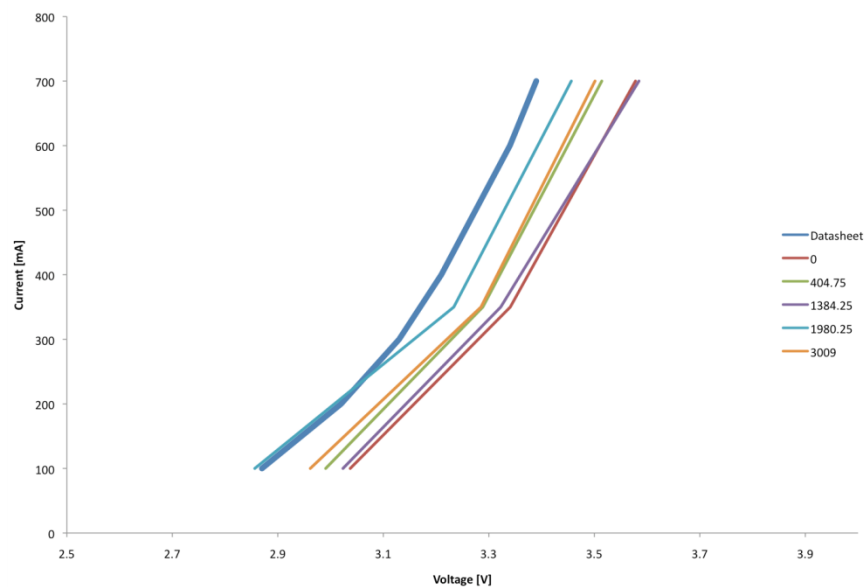
Figure 4.15: Plot of the average of Group B (Boards 3 and 4) I-V curves versus time.

The result of Group B's I-V curves not showing any degradation due to time may possibly indicate that an insufficient amount of time was spent aging these LEDs.

Unfortunately, due to time constraints of the research, a longer time was not possible. A summary of the results from this section can be found in Table 4.6.
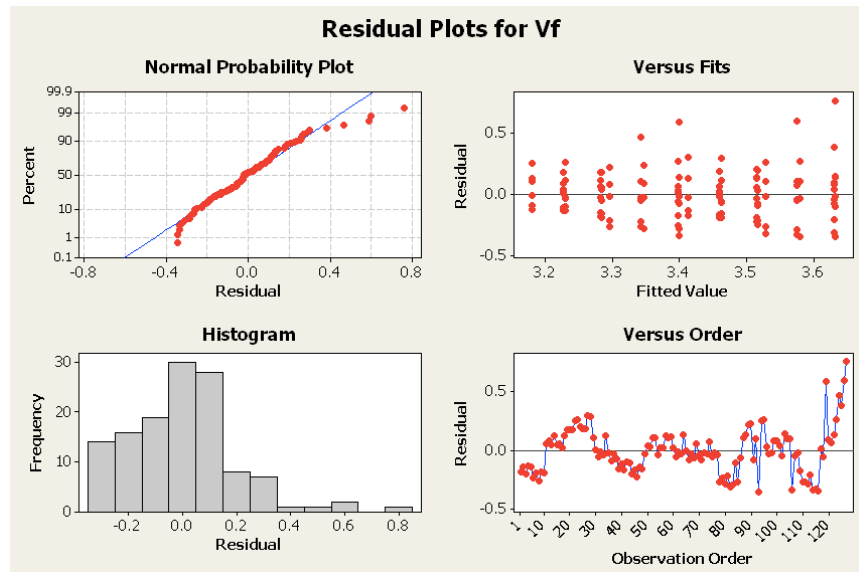
Figure 4.16: Residual plot from an One-Way ANOVA for Group B's (350mA aging current). The resulting plots show that the data is not normally distributed with a P-value of 0.040.

Table 4.6: Minitab analysis of Group B's I-V versus Time.

```
Kruskal-Wallis Test: Vf (@350mA) versus Time (@350mA)
Time
(@350mA)    N  Median  Ave Rank       Z
   0.00    27   3.393      78.3    2.48
 404.75    28   3.277      58.6   -0.72

1384.25    26   3.318      64.3    0.21
1980.25    24   3.227      49.5   -2.03
3009.00    20   3.260      62.9   -0.01
Overall   125              63.0

H = 8.59  DF = 4  P = 0.072


Kruskal-Wallis Test: Vf (@700mA) versus Time ((@700mA)
Time
((@700mA)   N  Median  Ave Rank       Z
   0.00    15   3.586      38.9    1.53
 404.75    14   3.502      29.4   -0.70
1384.25    13   3.543      35.5    0.64
1980.25    12   3.450      25.9   -1.36
3009.00    10   3.471      31.2   -0.24
Overall    64              32.5

H = 4.05  DF = 4  P = 0.399
```

Table 4.7: Summary of results for section 3.2.2

	350mA test current		700mA test current			
	P-value	**Result**	**P-value**	**Result**	**Conclusion**	**Expected?**
Control	0.422	Fail to reject H_0	0.644	Fail to reject H_0	I-V curves have not changed	Yes
Group A (Aging current 470mA)	0.001	Reject H_0	0.003	Reject H_0	I-V curves have changed	Yes
Group B (Aging current 350mA)	0.072	Possibly reject H_0	0.399	Fail to reject H_0	Most likely no change	

Chapter 5 – Conclusions and Recommendations

5.1 Data Acquisition System

Overall the data acquisition system worked well. It was able to accurately measure the forward voltage within short pulses. The measured values were verified against the datasheet of the tested chips. As mentioned in the design and testing section, there were numerous problems that were ultimately resolved which allowed for accurate testing. The DAQ design met the requirements of the measurement system. It was able to pulse a LED rapidly, collect many samples during this period, measure multiple chips, and test various currents. There was an issue with low current levels as discussed in section 4.1; however this was a small problem, which was resolved.

5.2 K-Factor Degradation

Overall the study was successful in showing that the K-factor does change. A statistically significant amount of change was detected between the initial calibration and the last three calibrations. Within 3000 hours, a 10.4% change in the K-factor was measured. This degradation was detected on Group B, which was aged at 115 °C. This elevated temperature was high, however only minimal changes in the I-V curves occurred. The I-V curves were monitored for shifts to the right or left which may indicate damage. During the aging process, Group B did not exhibit a statistically significant degradation even though the K-factor changed. The lack of change in the I-V

curves in Group B was strongly contrasted by the I-V curves from Group A. Group A was aged at average junction temperature of 145 °C. These LEDs degraded so rapidly that before the end of the second aging period, they had all failed. The results from these LEDs were not considered in the study.

The data collected from Group B turned out to be reasonably normally distributed. This result helped greatly in the analysis of the data. An analysis of Group B's results also indicated that the two boards that made the group were statistically different from each other despite receiving identical aging currents. At this time, the source of this difference is not fully understood; however it may have been due to the amount of damage done to the LEDs during assembly.

The boards that were analyzed in this study were assembled by hand. Surface mount chips were attached by using a soldering iron. This resulted in clearly damaged LEDs when comparing these boards to boards assembled using a reflow oven. This conclusion was drawing from comparing the I-V curves of both assembly methods relative to the values specified by Philips LumiLEDs. On a final note, datasheets from most LED manufactures only specify a single K-factor at one specified current. The LEDs used in this study were only specified at 350mA for K-factor by the manufacturer. Theory suggests that there should be a different K-factor for each current, and there indeed does as this study has shown. Having multiple current levels specified by the manufacturer would have greatly aided in verification of the collected data. The values collected at 350mA did indeed match the datasheet, however more data points for comparison would have been helpful.

5.3 Future Study

Currently there are no plans to continue this study. However, this study would greatly benefit from more aging. The LEDs that were tested may have a break-in period, which causes some tests to require a reset of data after the first 1000 hours. A data reset was not done in this test. Also, more calibration periods with shorter aging durations between calibrations would enhance this study. This would allow for a better understanding of the data trend and possibly allow the development of a model to forecast the K-factor for certain parameters.

This study also needs to be run in a way to isolate the current from the temperature. This would probably require a few aging currents and ovens to maintain the junction temperature at specific temperatures. This would require a lot more equipment; however, it would greatly assist in determining how the K-factor changes with respect to time.

The PCBs that were used in this study should have been reflowed. Ultimately there were some boards assembled using a reflow oven. These boards were fabricated from metal-cored PCB late into the study, which meant there was not enough time to collect data. However, even FR-4 with reflow soldering would greatly reduce the damage to these LEDs during assembly. Due to the damage of hand soldering, there is no way to tell if the K-factor changes that were seen are due to degradation or because of the hand soldering.

The data acquisition had many shortcomings that hindered the collection of data. Due to such a time constraint, LabView was used. Using LabView caused many

problems that could have been avoided simply by using an imbedded processor. LabView had many runtime errors because of the multiple requests to take measurements. This would cause errors that would crash the collection system; unfortunately there was no way to bypass this type of error with a simple redesign. Also, LabView was painfully slow at collecting data. If this type of data acquisition system is redesigned, LabView should not be used.

Finally, a better extrapolation model should be used to find the forward voltage during calibration. Currently a simple linear fit is being used. A model that incorporated more of the solid-state physics and heat transfer would provide a superior model. This model, if possible should include the rise time associated with the driver. The rise time could be improved with redesign of the circuitry; however there will always be a rise time and this is why the model should include it.

References

[1] Cree. "Cree Breaks 200 Lumen Per Watt Efficacy Barrier." 3 Feb 2010. 14 May 2010. <http://www.cree.com/press/press_detail.asp?i=1265232091259>.

[2] Cree. Cree XLamp LED Thermal Management. 2006. Jan 2009. <http://www.cree.com/products/pdf/XLampThermalManagement.pdf>.

[3] Mehmet Arik, Charles Becker, Stanton Weaver, and James Petroski. "Thermal Management of LEDs: Package to System." 2004. Jan 2009. <http://lib.semi.ac.cn:8080/tsh/dzzy/wsqk/SPIE/vol5187/5187-64.pdf>.

[4] Alliance for Solid-State Illumination Systems and Technologies (ASSIST). LED Life for General Lighting: Definition of Life, Volume 1, Issue 1. New York Lighting Research Center, Rensselaer Polytechnic Institute. 2005. May 2010.

[5] United States. Department of Energy. Solid state Lighting Energy Star Requirements. 9 Dec 2007. Dec 2009. <http://www.energystar.gov/ia/partners/prod_development/new_specs/downloads/SSL_FinalCriteria.pdf>.

[6] Underwriters Laboratories Inc. UL 8750: Light-emitting diode Equipment for Use in Lighting Products. Standard for Safety. 25 Jan 2010. May 2010. 34.

[7] Shatil Haque (LumiLEDs). "Packaging of Power LEDs Using Thermosonic Bonding of Au-Au Interconnects." California Polytechnic State University. 14 April 2009.

[8] Incropera, DeWitt, Bergman, and Lavine. Introduction to Heat Transfer. Wiley. 2007. 6-7 & 98-99.

[9] Electronic Industries Association. Integrated Circuits Thermal Measurement Method – Electrical Test Method (Single Semiconductor Device). December 1995. November 2009. < http://www.jedec.org/standards-documents/results/taxonomy:2480>.

[10] Y.Xi and E. F. Schubert. "Junction-temperature measurement in GaN ultraviolet light-emitting diodes using diode forward voltage method." *Applied Physics Letters*. Volume 85, Number 12. September 2004. September 2009.

[11] Vektrex Electronic Systems Inc. "Measuring LED Junction Temperature. 2009. <http://www.vektrex.com/Support/kb/In-Situ%20Junction%20Temperature%20.pdf>.

[12] Fluke. <u>2x4 wire resistance simplifies precision measurements</u>. 2006. Feb 2010.
<http://support.fluke.com/calibration-
sales/Download/Asset/2557732_6200_ENG_A_W.PDF >.

[13] Gu, Y., N. Narendram, and J.P. Freyssiner. "White LED performance." Fourth
International Conference on Solid State Lighting, Proceedings of SPIE 5530.
Bellingham, WA: International Society of Optical Engineers. 2004.

[14] Buso, Simone, Giorgio Spiazzi, Matteo Meneghini, and Gaudenzio Meneghesso.
"Performance Degradation of High-Brightness Light-emitting diodes Under DC and
Pulsed Bias." IEEE Transactions on Device and Materials Reliability. Vol. 8, No. 2,
June 2008. Jan 2010.

[15] Cao, X. A., Stokes, P. M. Sandvik, S. F. LeBoeuf, J. Kretchmer, and D. Walker.
"Diffusion and Tunneling Currents in GaN/InGaN Multiple Quantum Well Light-
Emitting Diodes." *IEEE Electron Device Letters*. Vol. 23, No. 9, September 2002.
April 2010.

[16] Meneghini, Matteo, Lorenzo-Roberto, Gaudenzio Meneghesso, and Enrico Zanoni.
"A Review on the Reliability of GaN-Based LEDs." *IEEE Transactions on Device
and Materials Reliability*, Vol 8, No 2, June 2008. November 2009.

[17] Sze, S. <u>Physics of Semiconductor Devices</u>. 2nd Edition, Wiley, 1984. May 2009.

[18] Philips LumiLEDs. <u>LUXEON Rebel Thermal Measurement Guidelines</u>. Application
Brief AB33. 2008. <http://www.philipslumileds.com/pdfs/AB33.pdf>.

[19] Philips LumiLEDs. <u>LUXEON Rebel Assembly and Handling Information.</u>
Application Brief AB32. 2008. <http://www.philipslumileds.com/pdfs/AB32.pdf>.

[20] Wikipedia. "FR-4." <http://en.wikipedia.org/wiki/FR-4>. Accessed February 2010.

[21] Philips LumiLED. <u>Power light source LUXEON Rebel</u>. Technical Datasheet DS56.
This datasheet has been replaced by DS63. 2007.

[22] Philips LumiLEDs. <u>LUXEON Rebel Illumination Portfolio</u>. Technical Datasheet
DS63. 2010.

[23] Levine, David M., Patricia P. Ramsey, and Robert K. Smidt. <u>Applied Statistics for
engineers and scientists</u>.   New Jersey: Prentice-Hall Inc, 2001.

Appendices

Appendix A – Data Acquisition System

A.1 Schematic

Unfortunately, I did not know how to use the sheet function of the software when I made the circuit.   Each sub-circuit is separated onto a separate appendix page.
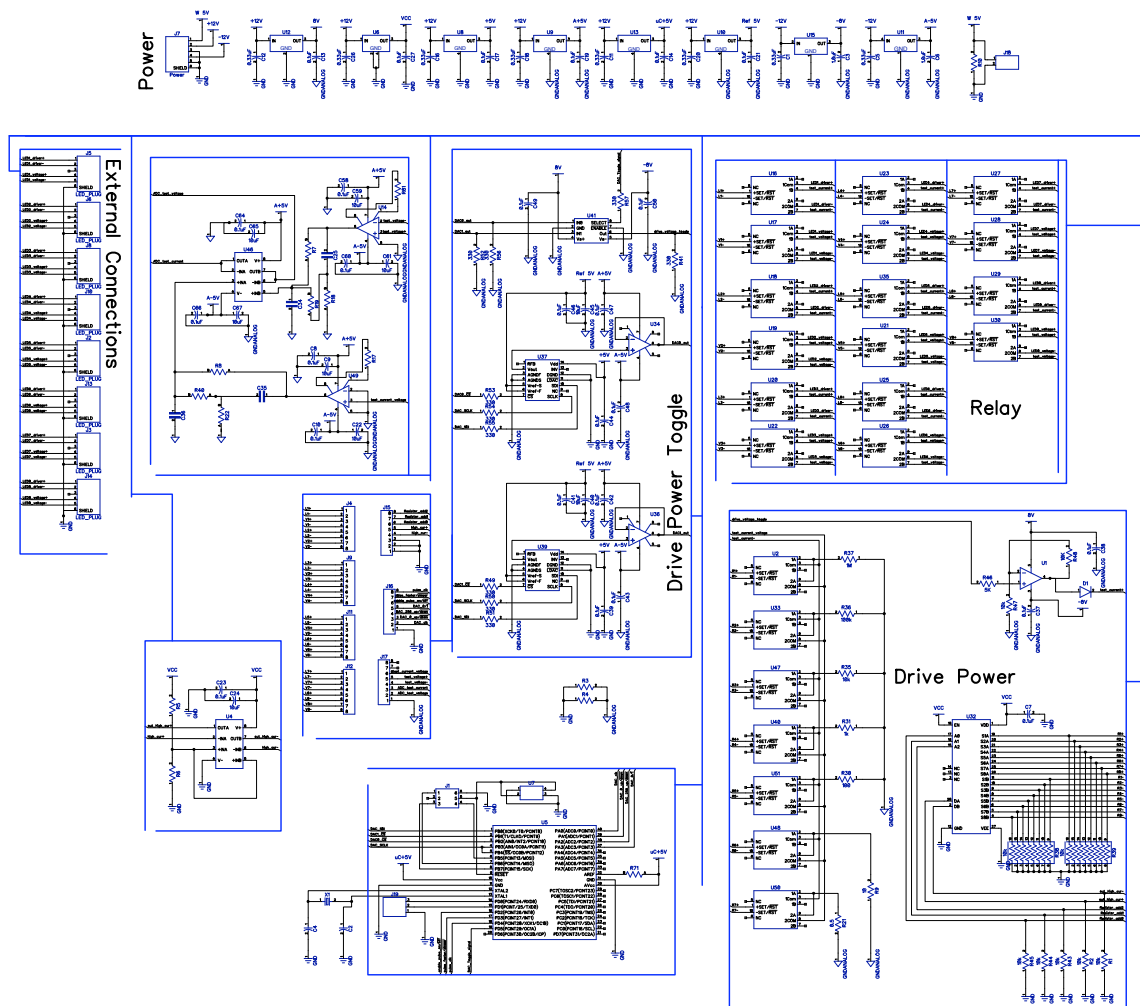
Overview of custom data acquisition interface board
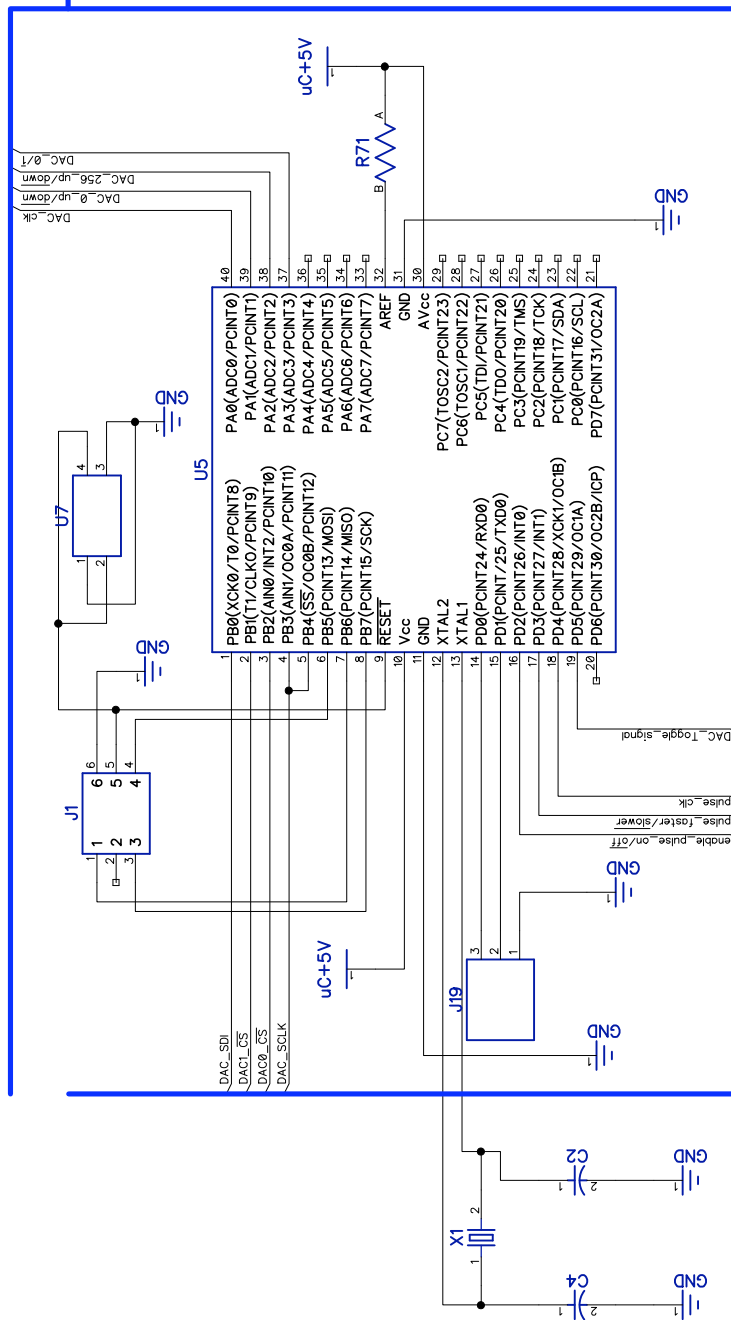
Schematic of microcontroller circuit
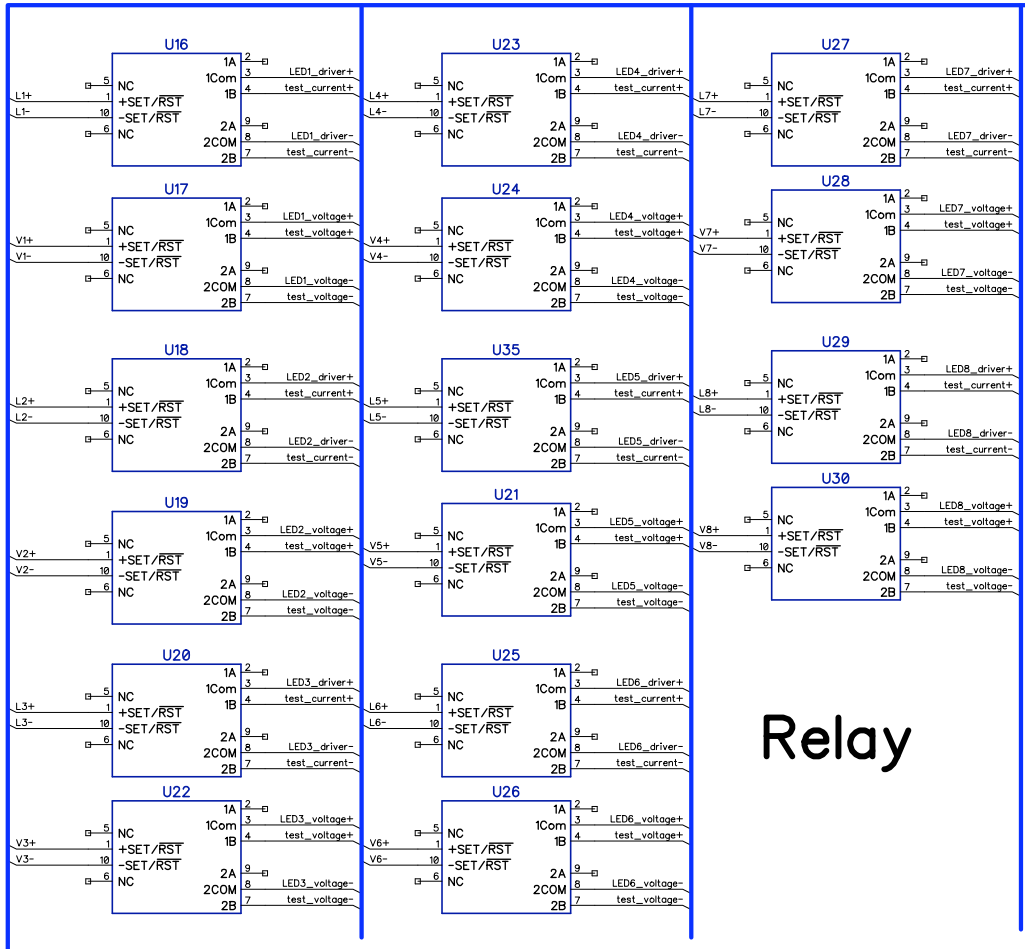
Relay

Schematic of LED multiplexing relays
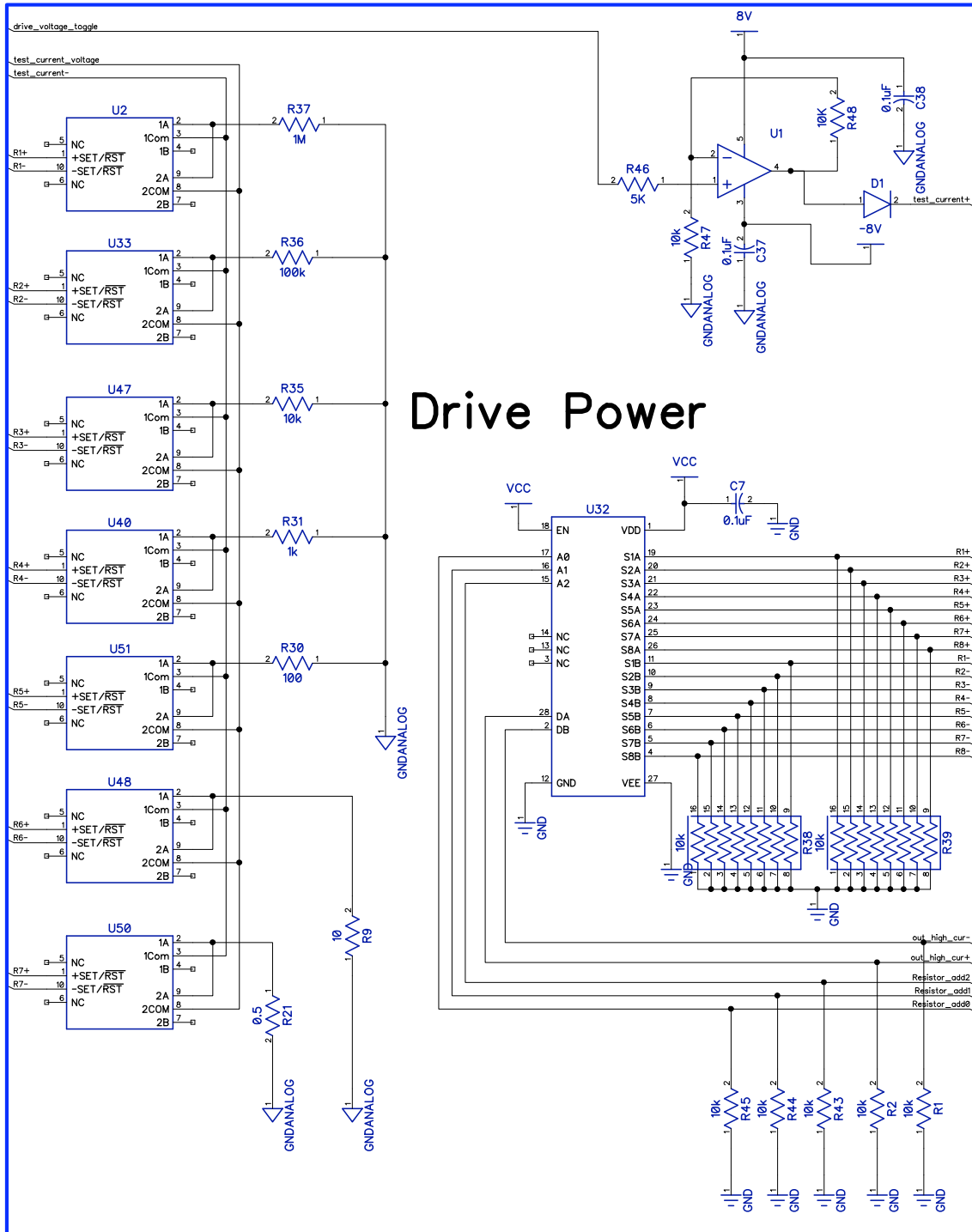
Schematic driver circuit with current range selection relays
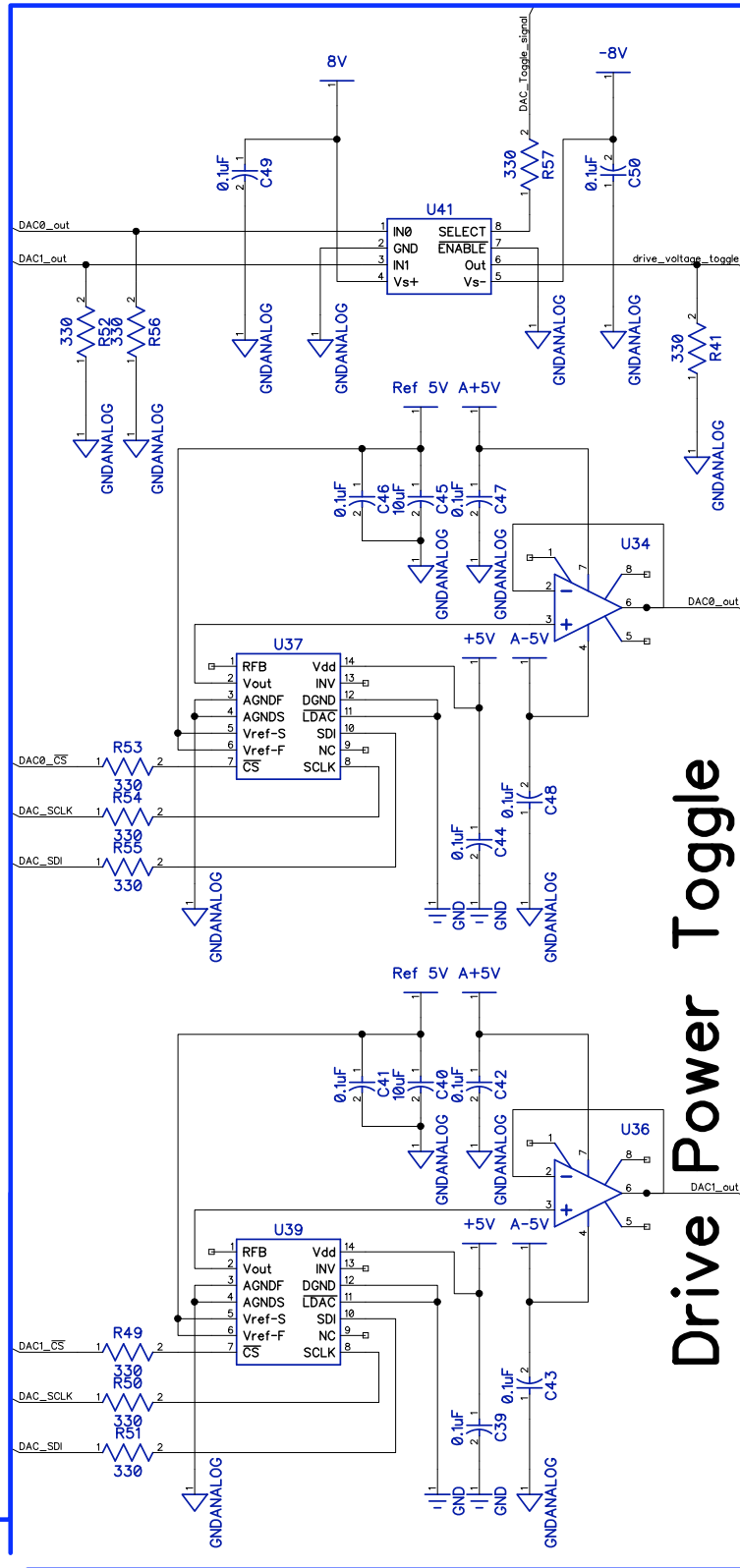
Schematic to toggle LEDs on and off.
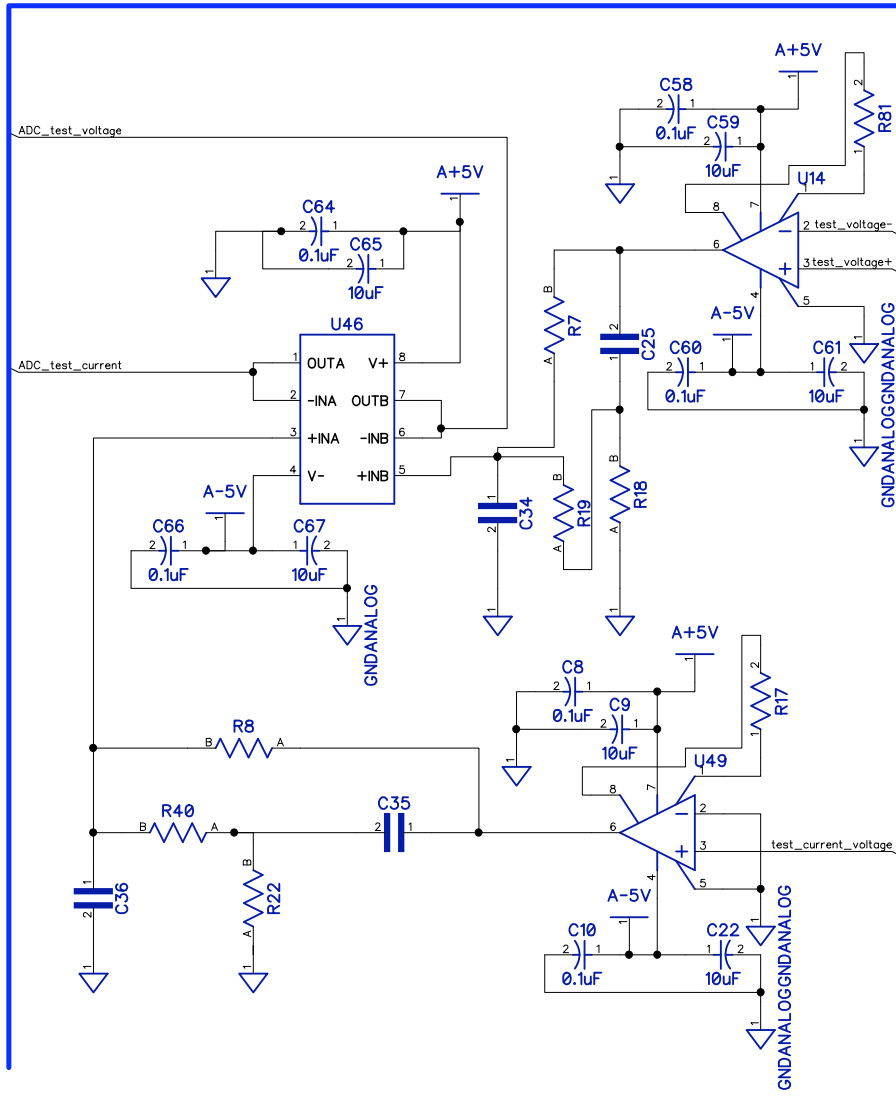
Schematic of optional analog band-pass filter

Schematic of terminal blocks for connecting with NI PCI DAQ card

Schematic of LED connectors

Schematic of power distribution.

A.2 Layout

Top layer of the PCB layout for interface board

Bottom layer of PCB layout for interface board

A.3 Pinout from Interface board to NI Breakout Boards

Power Test — Board A (Analog Inputs)

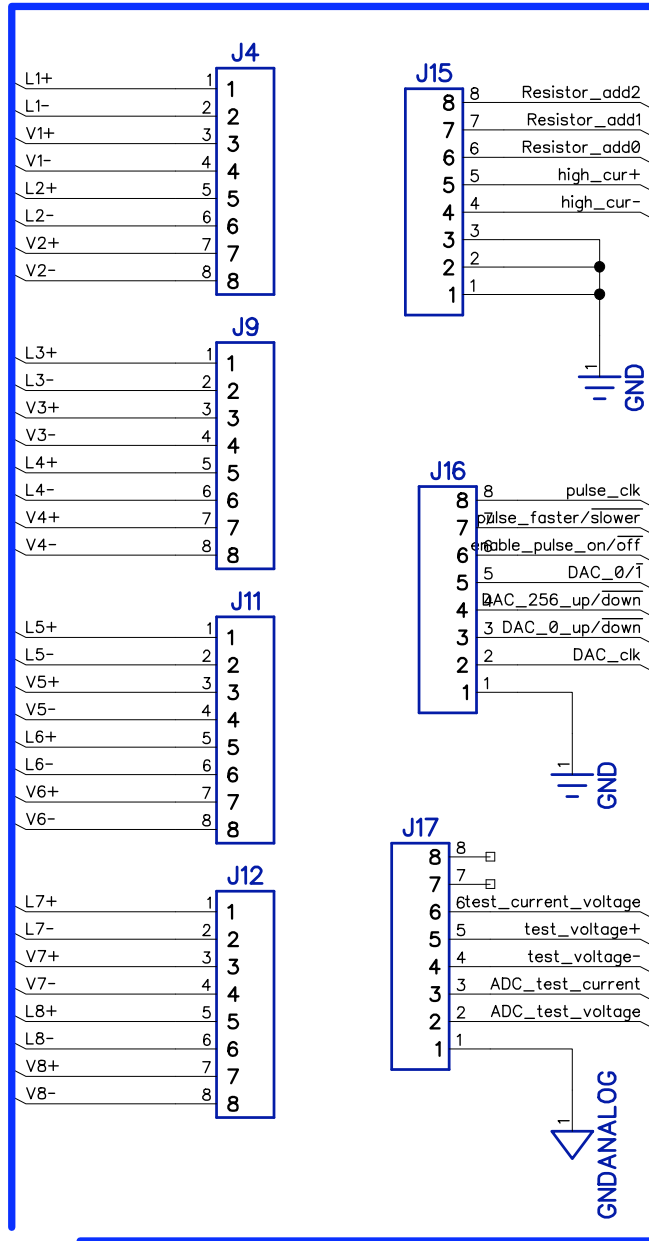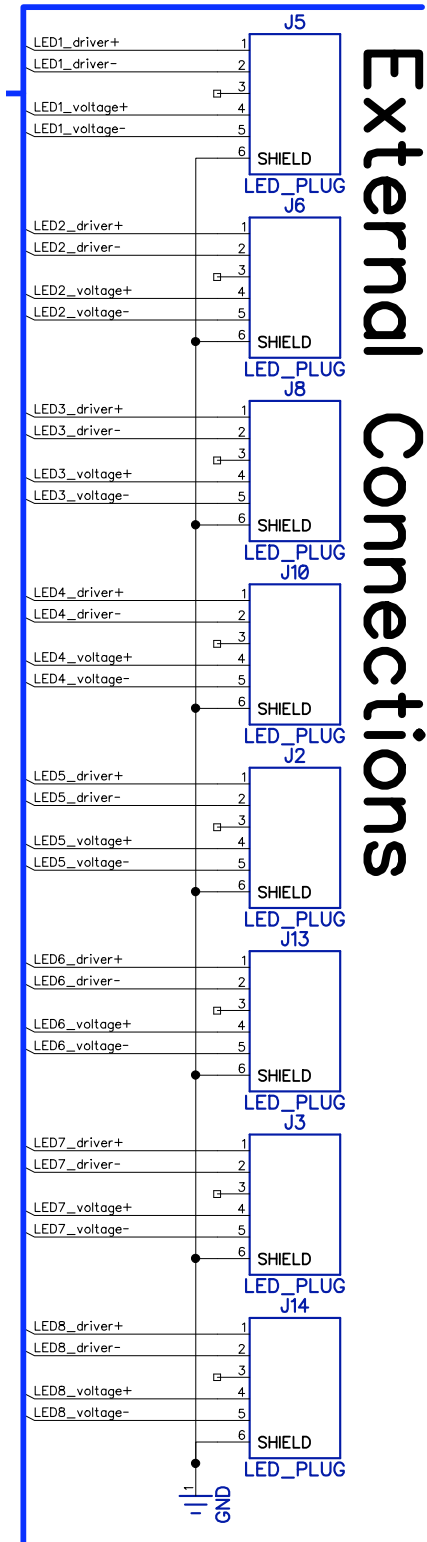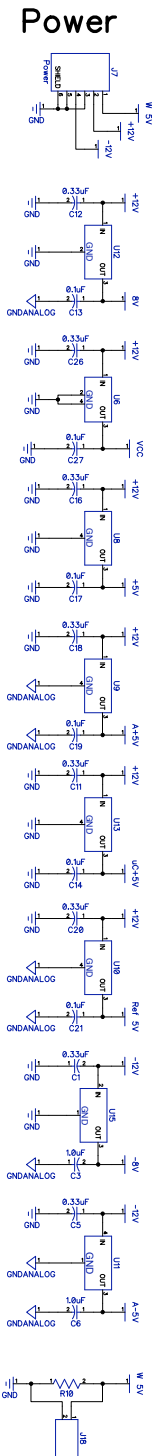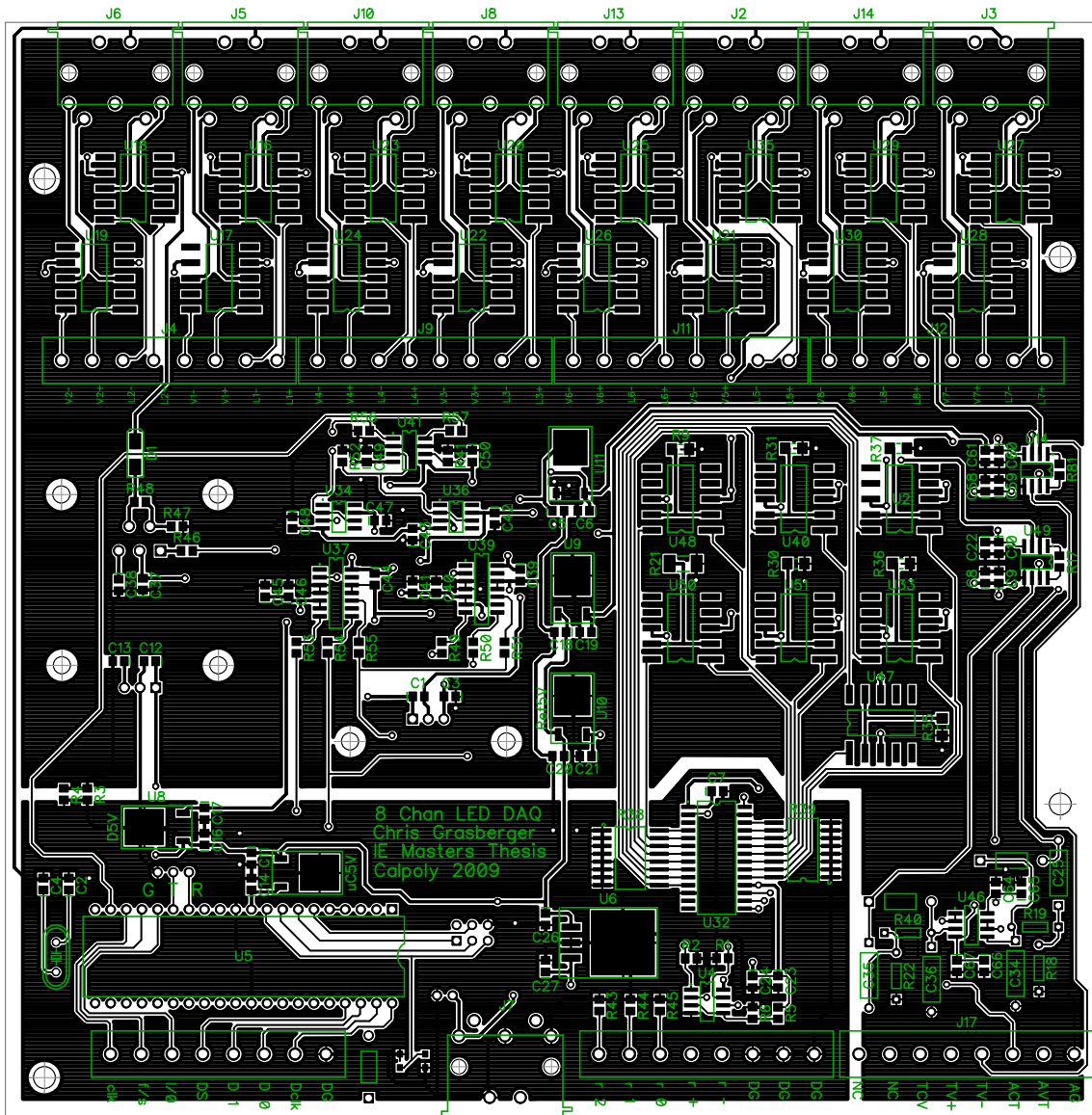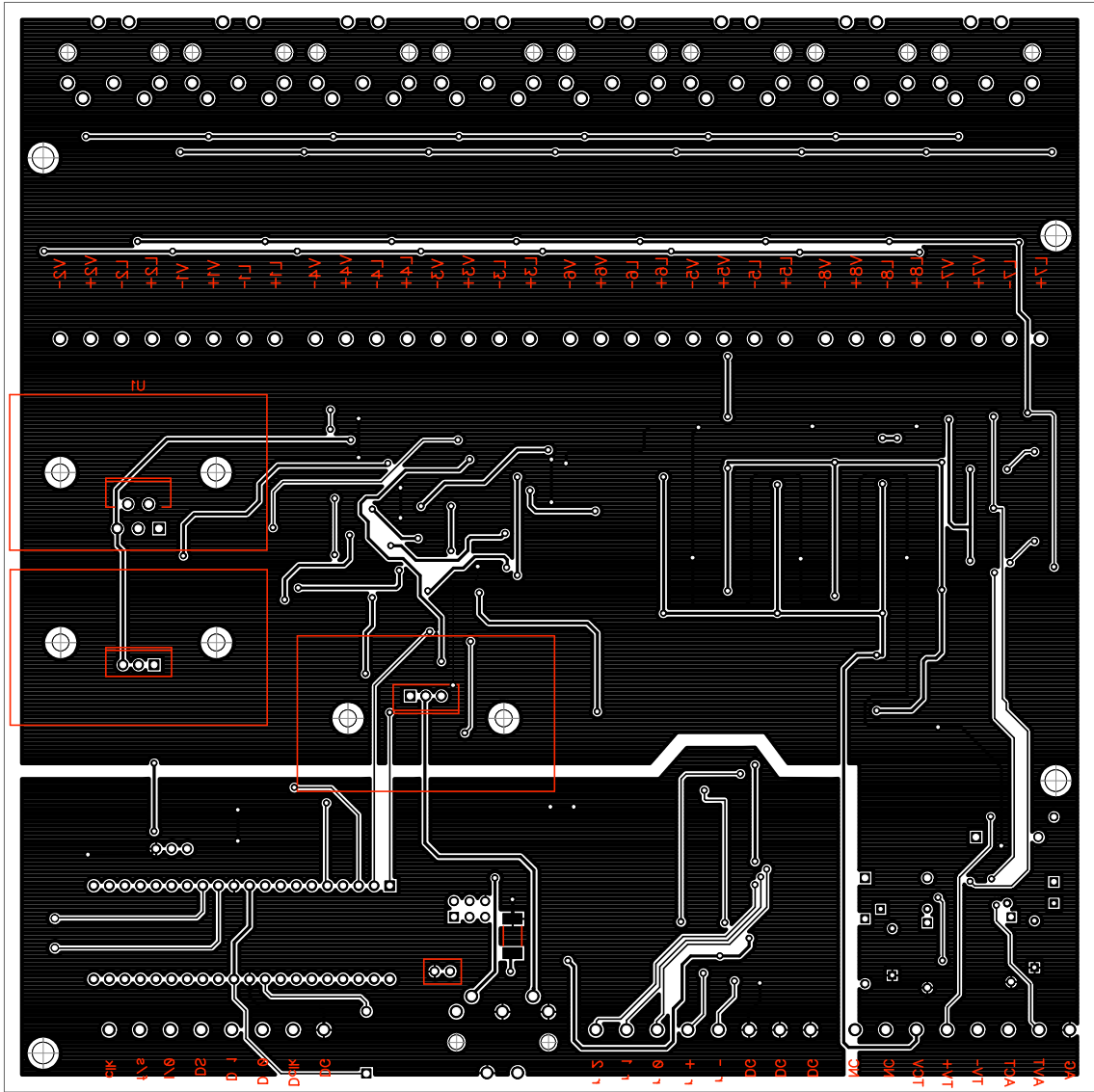| Bus	Pin	Signal	Note
A	68	AI 0	
A	34	AI 8	
A	67	AI GND	
A	33	AI 1	
A	66	AI 9	
A	32	AI GND	
A	65	AI 2	
A	31	AI 10	
A	64	AI GND	
A	30	AI 3	
A	63	AI 11	
A	29	AI GND	
A	62	AI SENSE	
A	28	AI 4	
A	61	Ai 12	
A	27	AI GND	
A	60	AI 5	
A	26	Ai 13	Thermocouple
A	59	AI GND	
A	25	AI 6	RED
A	58	AI 14	YELL
A	24	Ai GND	
A	57	AI 7	DAC 0 Voltage

Correct Test — Board B (Analog Inputs)

Bus	Pin	Signal	Note
B	68	AI 16	
B	34	AI 24	
B	67	AI GND	
B	33	AI 17	
B	66	AI 25	
B	32	AI GND	
B	65	AI 18	
B	31	AI 26	
B	64	AI GND	
B	30	AI 18	
B	63	AI 27	
B	29	AI GND	
B	62	AI SENSE 2	
B	28	Ai 20	TCV+ Resistor Voltage Pre Opamp
B	61	AI 28	TCVG
B	27	AI GND	
B	60	AI 21	TV+ LED Voltage Pre OPAMP DIFFERENTIAL
B	26	AI 29	TV-
B	59	AI GND	
B	25	Ai 22	ACT+ Current Test Post Opamp
B	58	AI 30	ACTG
B	24	AI GND	AI GND
B	57	Ai 23	AVT+ Voltage Test Post Opamp
B	23	AI 31	AVTG

Board A (Digital / LED RELAY A)

Bus	Pin	Signal	Type
A	12	DGND	
A	46	P2.3	analog trigger
A	13	DGND	
A	47	P0.3	V2+ LED RELAY A
A	14	5V	V2- LED RELAY A
A	48	P0.7	
A	15	GND	
A	49	P0.2	L2+ LED RELAY A
A	16	P0.6	L2- LED RELAY A
A	50	DGND	
A	17	P0.1	V1+ LED RELAY A
A	51	P0.5	V1- LED RELAY A
A	18	DGND	
A	52	P0.0	L1+ LED RELAY A
A	19	P0.4	L1- LED RELAY A
A	53	GND	
A	20	APPFI 0	
A	54	NC	
A	21	NC	
A	55	NC	
A	22	NC	
A	56	AI GND	

Board B (Digital / LED RELAY C)

Bus	Pin	Signal	Type
B	12	DGND	
B	46	P0.27	V4+ LED RELAY C
B	13	DGND	
B	47	P0.11	V6+ LED RELAY C
B	14	5V	V6- LED RELAY C
B	48	P0.15	
B	15	DGND	
B	49	P0.10	L6+ LED RELAY C
B	16	P0.14	L6- LED RELAY C
B	50	DGND	
B	17	P0.9	V5+ LED RELAY C
B	51	P0.13	V5- LED RELAY C
B	18	DGND	
B	52	P0.8	L5+ LED RELAY C
B	19	P0.12	L5- LED RELAY C
B	53	DGND	
B	20	APFI 1	
B	54	NC	
B	21	NC	
B	55	NC	
B	22	NC	
B	56	AI GND	

Board A (Digital / RES RELAY)

Bus	Pin	Signal	Type
A	1	P2.6	Dclk — DIGITAL
A	35	DGND	D 0 — DIGITAL
A	2	P2.4	
A	36	DGND	D 1 — DIGITAL
A	3	P2.1	DS — DIGITAL
A	37	P2.0	DGND — DIGITAL
A	4	DGND	I/O — DIGITAL
A	38	P1.7	f/s — DIGITAL
A	5	P1.5	clk — DIGITAL
A	39	P2.7	1k- — RES RELAY
A	6	P1.5	1k+ — RES RELAY
A	40	P2.5	
A	7	DGND	100- — RES RELAY
A	41	P1.4	100+ — RES RELAY
A	8	5V	
A	42	P1.3	10- — RES RELAY
A	9	DGND	10+ — RES RELAY
A	43	P1.2	
A	10	P1.1	0.5- — RES RELAY
A	44	DGND	0.5+ — RES RELAY
A	11	P1.0	
A	45	P2.2	

Board B (LED RELAY B / LED RELAY D)

Bus	Pin	Signal	Type
B	1	P0.30	V4- LED RELAY B
B	35	DGND	L4+ LED RELAY B
B	2	P0.28	
B	36	DGND	L4- LED RELAY B
B	3	P0.25	V3+ LED RELAY B
B	37	P0.24	V3- LED RELAY B
B	4	DGND	L3+ LED RELAY B
B	38	P0.23	L3- LED RELAY B
B	5	P0.22	V8+ LED RELAY D
B	39	P0.31	V8- LED RELAY D
B	6	P0.21	L8+ LED RELAY D
B	40	P0.29	
B	7	DGND	L8- LED RELAY D
B	41	P0.20	
B	8	5V	
B	42	P0.19	V7+ LED RELAY D
B	9	DGND	V7- LED RELAY D
B	43	P0.18	
B	10	P0.17	
B	44	DGND	L7+ LED RELAY D
B	11	P0.16	L7- LED RELAY D
B	45	P0.26	

A.4 LabView Interface Screenshots
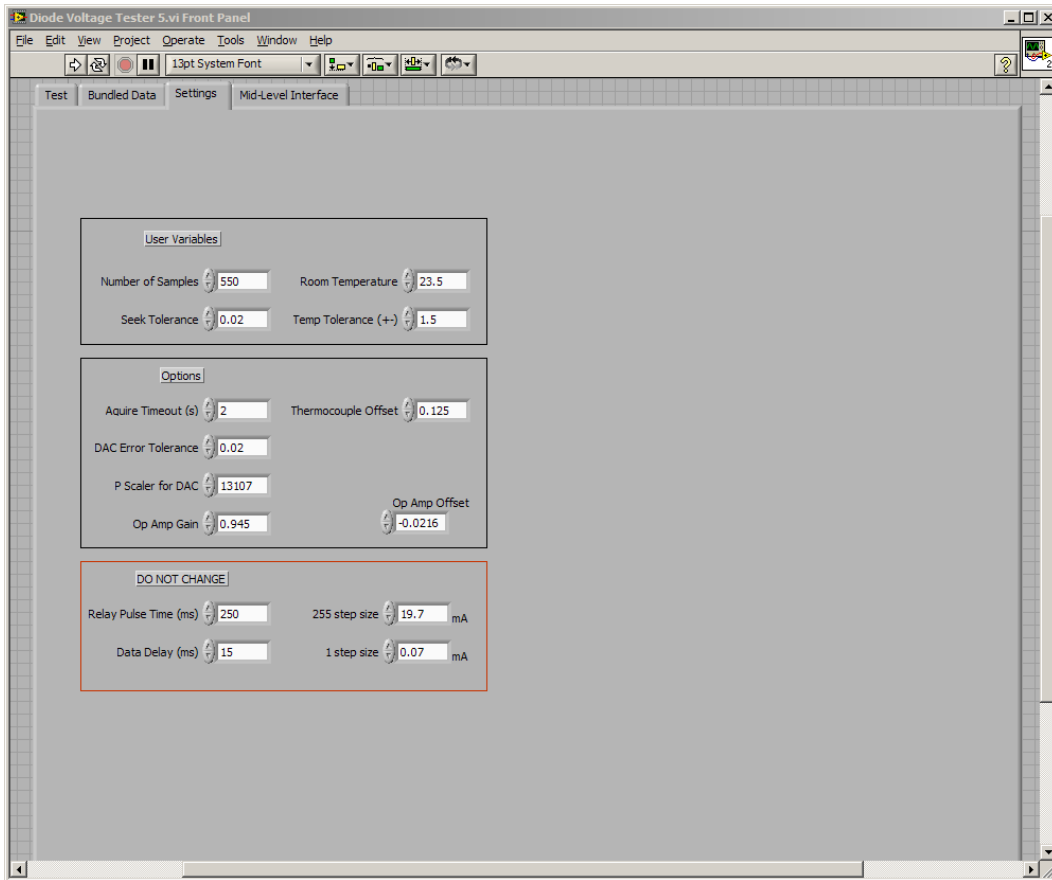
Screen shot showing the settings tab. This tab can be used to adjust timing, thermocouple offsets, and other values.
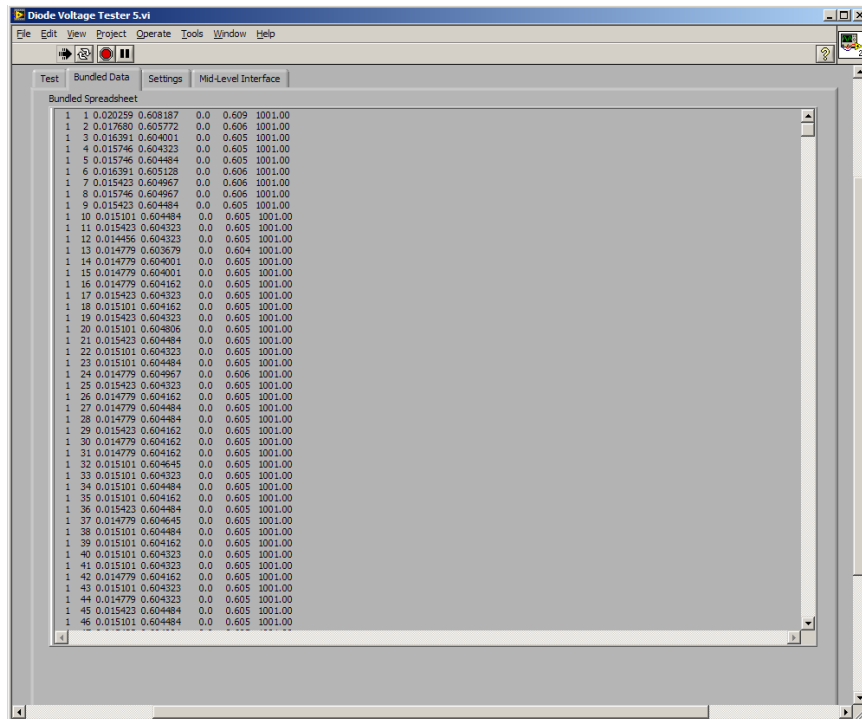
Screen shot of the "Bundled Data" tab. Each time the "Next Data Group" button is pressed, the collected data is added to the Bundled Data table as a set of 6 columns next to the one shown above.
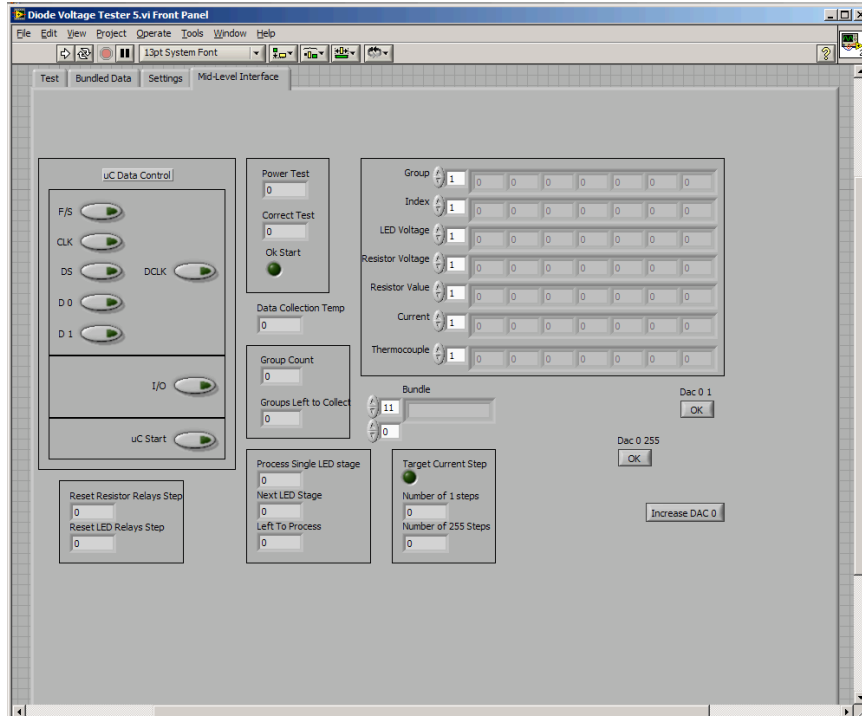
This is the mid-level interface tab. This tab shows the primary tools used in the main user interface on the test tab.

A.5 Bill of Materials

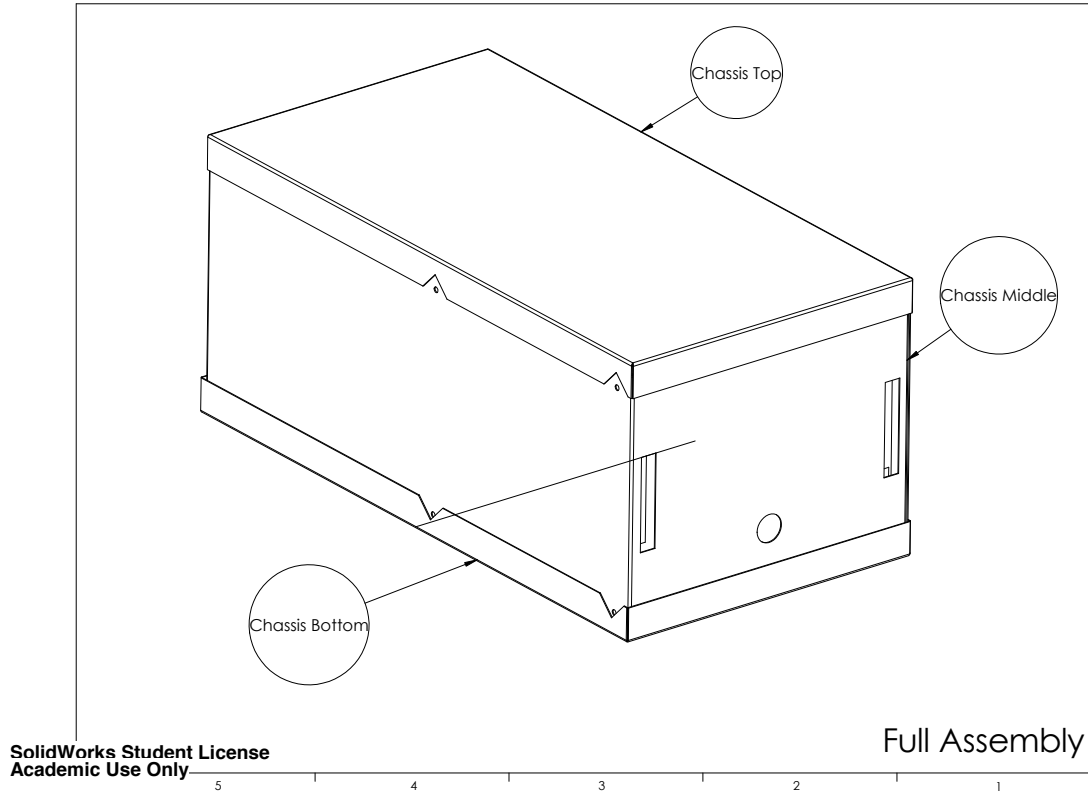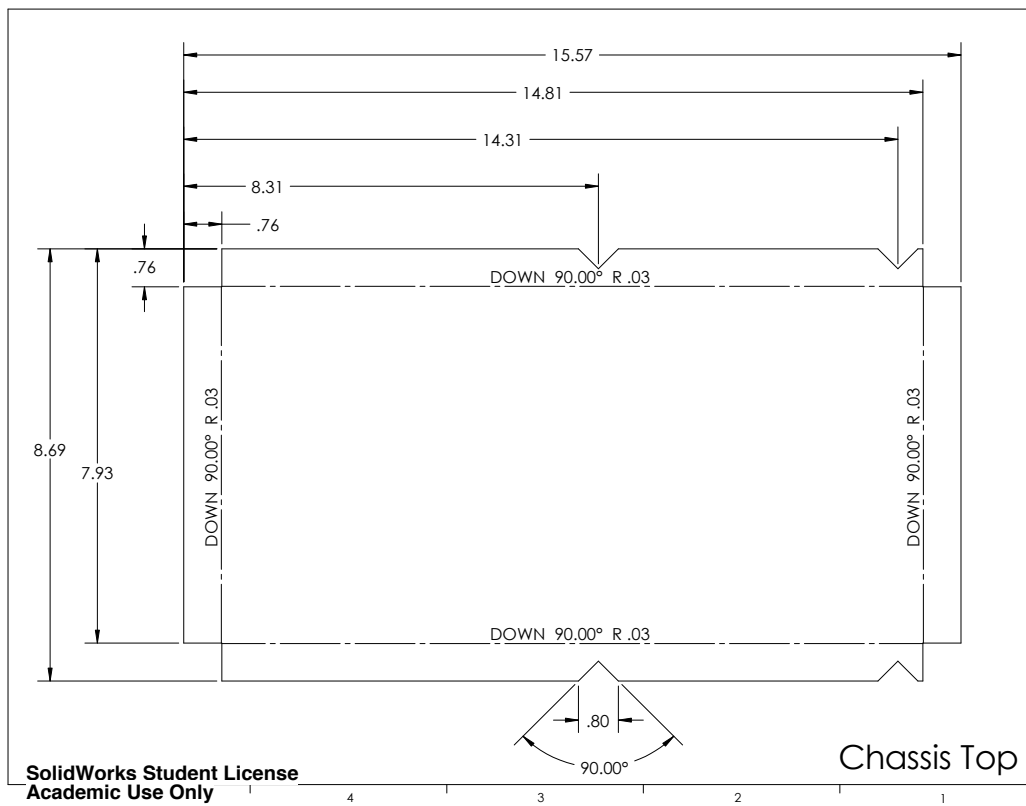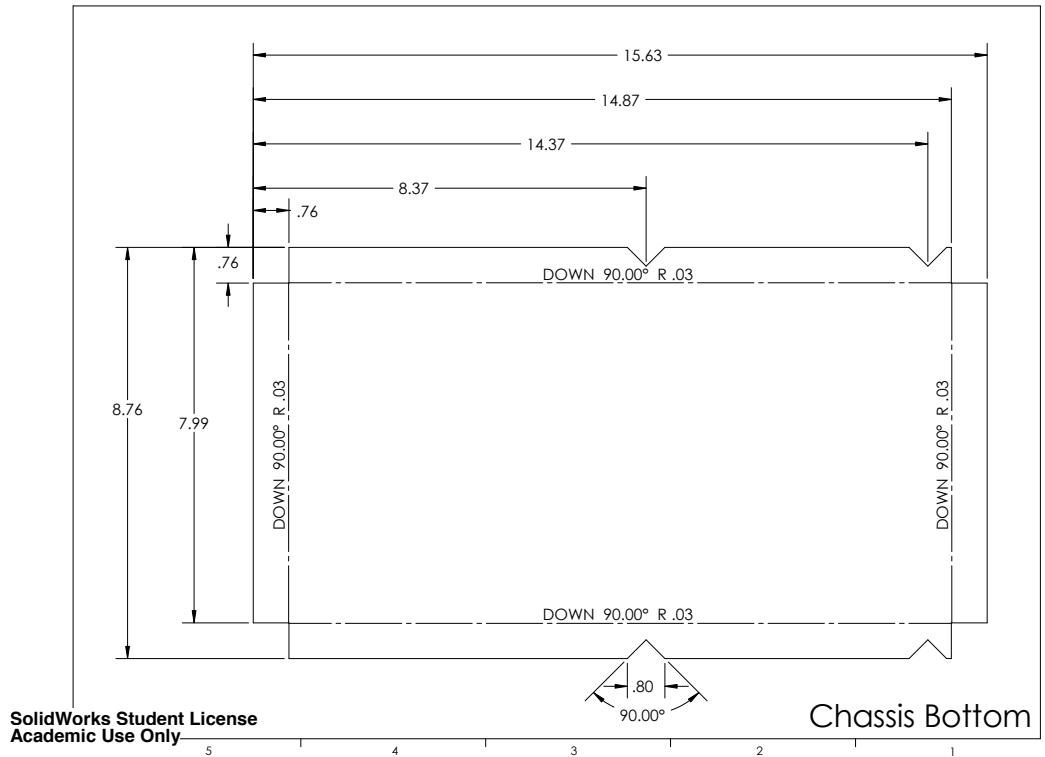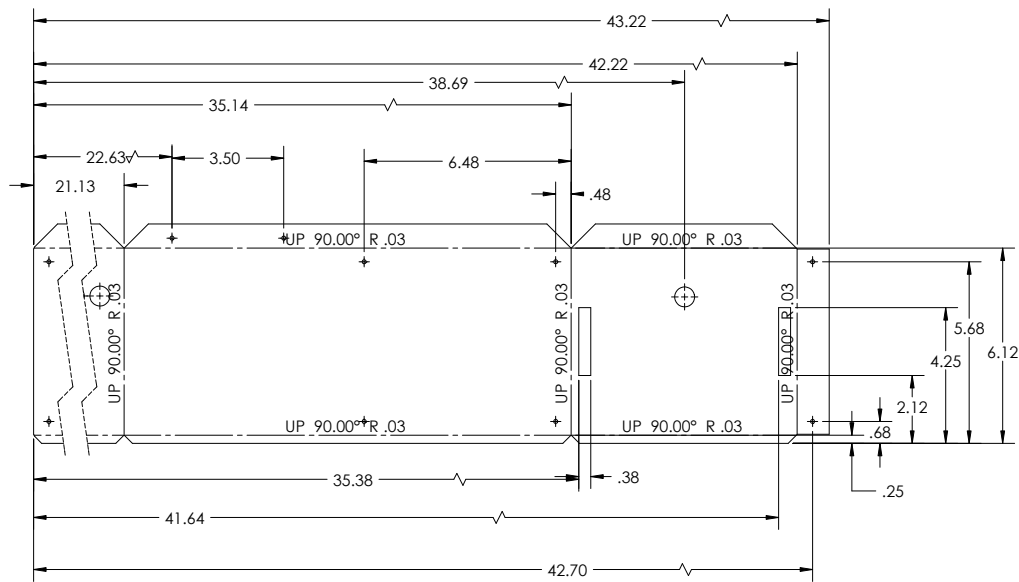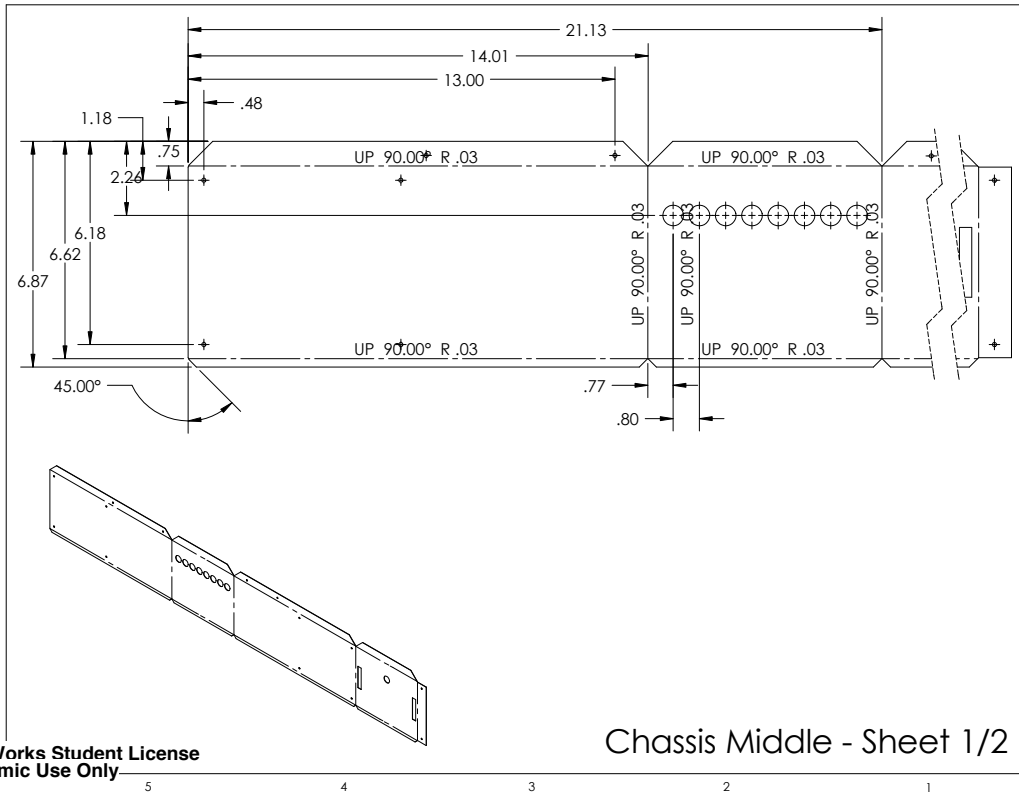| RefDes	Value	Digikey #	Description	Manufacture	Manufactuer #
C1, C12, C14, C16, C18, C2, C20, C5	0.33uF	PCC1817CT-ND	CAP .33UF 16V CERAMIC X7R 0805	Panasonic - ECG	ECJ-2YB1C334K
C10, C11, C13, C15, C17, C19, C21, C26, C27, C29, C32, C33, C37, C38, C39, C41, C42, C43, C44, C46, C47, C48, C49, C50, C51, C53, C55, C57, C58, C60, C64, C66, C7, C8	0.1uF	PCC1828CT-ND	CAP .1UF 25V CERAMIC X7R 0805	Panasonic - ECG	ECJ-2VB1E104K
C22, C40, C45, C59, C61, C65, C67, C9	10uF	490-3347-1-ND	CAP CER 10UF 16V Y5V 0805	GRM21BF51C106ZE15L	Murata
C24	2.2uF	PCC2322CT-ND	CAP CERAMIC 2.2UF 16V X5R 0805	Panasonic - ECG	ECJ-2FB1C225K
C28, C3, C4, C52, C56, C6	1.0uF	PCC2319CT-ND	CAP CERAMIC 1UF 25V X5R 0805	Panasonic - ECG	ECJ-2FB1E105K
R10, R11, R12, R13, R41, R49, R50, R51, R52, R53, R54, R55, R56, R57, R58, R59, R60, R62, R63, R64	330	P330ACT-ND	RES 330 OHM 1/8W 5% 0805 SMD	Panasonic - ECG	ERJ-6GEY331V
R15, R16, R38, R39	10k	767-163-R10KP-ND	RES NET 8RES 10K OHM 16PIN SMD	CTS	767163103GP
R21	0.5	CSRN10.25FICT-ND	RES .25OHM 3/4W 1% 2010 SMD	Stackpole	CSRN 1 0.25 1% I
R23, R24, R25, R43, R44, R45, R47	10k				
R26, R27, R28, R29	10	CRT1206-BY-10R0ELFCT-ND	RES 10 OHM 1/8W .1% 1206 SMD	Bournes	CRT1206-BY-10R0ELF
R30	100	RNCS32T9100BICT-ND	RES 1/8W 100 OHM 0.1% 1206	Stackpole	RNCS 32 T9 100 0.1% I
R31	1k	RNCS32T91KBICT-ND	RES 1/8W 1K OHM 0.1% 1206	Stackpole	RNCS 32 T9 1K 0.1% I
R32, R33, R34, R6, R7, R8, R9	470	P470CCT-ND	RES 470 OHM 1/8W 1% 0805 SMD	Panasonic - ECG	ERJ-6ENF4700V
R35	10k	CRT1206-BY-1002ELFCT-ND	RES 10K OHM 1/8W .1% 1206 SMD	Bournes	CRT1206-BY-1002ELF
R36	100k	CRT1206-BY-1003ELFCT-ND	RES 100K OHM 1/8W .1% 1206 SMD	Bournes	CRT1206-BY-1003ELF
R37	1M	CRT1206-BY-1004ELFCT-ND	RES 1.0M OHM 1/8W .1% 1206 SMD	Bournes	CRT1206-BY-1004ELF
R46	5K	RMCF1/105.1KJRCT-ND	RES 5.1K OHM 1/8W 5% 0805 SMD	Stackpole	RMCF 1/10 5.1K 5% R
U1		LM675T-ND	IC OP AMP POWER TO-220-5	National	LM675T/NOPB
U14, U49		AD623ARZ-ND	IC AMP INSTR SGL R-R OUT 8-SOIC	Analog Devices	AD623ARZ
U2, U17, U16, U18, U19, U20, U21, U22, U23, U24, U25, U26, U27, U28, U29, U31, U33, U35, U40, U47, U48, U50, U51		255-2284-5-ND	RELAY LATCH 2A 5VDC LO PRO SMD	Panasonic Electric	TQ2SS-L-5V
U32, U38		DG407DY-ND	IC MUX ANALOG 8:1 28-SOIC	Interstil	DG407DY
U34, U36		OPA27GU-ND	IC LN PRECISION OPAMP 8 SOIC	Texas Instrumetns	OPA27GU
U37, U39		296-18030-5-ND	IC DAC 16-BIT V-OUT 14-SOIC	Texas Instrumetns	DAC8311D
U41		AD8180ARZ-ND	IC MUX SWITCHING 2:1 8-SOIC	Analog Devices	AD8180ARZ
U42, U45		LTC1864CS8#PBF-ND	IC A/D CONV 1CH 16BIT 8-SOIC	Linear Technology	LTC1864CS8#PBF
U44		ATMEGA2560-16AU-ND	IC AVR MCU 256K 16MHZ 100TQFP	Atmel	ATMEGA2560-16AU
U46		296-21651-1-ND	IC OPAMP CMOS DUAL 12V 8-SOIC	Texas Instrumetns	OPA2727AIDR
U6		296-1020-1-ND	IC BUS BUFF TRI-ST QD 14SOICN	Texas Instrumetns	SN74ABT126DR
U15		497-7760-1-ND	IC REG VLDO 250MA 3.5V DPAK	ST Micro	L4931ABDT35TR
U3		296-21933-1-ND	IC POS-VOLT REG 1.5A 8V D2PAK-3	Texas Instrumetns	UA7808CKTTR
U7, U8, U9, U10		296-19755-1-ND	IC VOLT REG POS 5V .5A DPAK	Texas Instrumetns	UA78M05CKVURG3
U4		MC7908CD2TGOS-ND	IC REG NEG VOLT 1A 8V D2PAK	ON Semiconductor	MC7908CD2TG
U11, U5		MC79M05CDTRKGOSCT-ND	IC REG VOLT NEG 500MA 5V DPAK	ON Semiconductor	MC79M05CDTRKG
X1	16MHz	631-1108-ND	CRYSTAL 16.0 MHZ 20PF	Fox Electronics	FOXSLF/160-20

A.6 Chassis Design

Full Assembly

Chassis Bottom

15.63

14.87

14.37

8.37

.76

.76

DOWN 90.00° R .03

8.76

7.99

DOWN 90.00° R .03

DOWN 90.00° R .03

DOWN 90.00° R .03

.80

90.00°

5   4   3   2   1

Chassis Top

15.57

14.81

14.31

8.31

.76

.76

DOWN 90.00° R .03

8.69

7.93

DOWN 90.00° R .03

DOWN 90.00° R .03

DOWN 90.00° R .03

.80

90.00°

4   3   2   1

84

Chassis Middle - Sheet 1/2

21.13
14.01
13.00
.48
1.18
.75
2.28
6.18
6.62
6.87
UP 90.00° R .03
UP 90.00° R .03
UP 90.00° R .03
UP 90.00° R .03
UP 90.00° R .03
UP 90.00° R .03
UP 90.00° R .03
UP 90.00° R .03
45.00°
.77
.80

5   4   3   2   1

Chassis Middle - Sheet 2/2

43.22
42.22
38.69
35.14
22.63
3.50
6.48
21.13
.48
UP 90.00° R .03
UP 90.00° R .03
UP 90.00° R .03
UP 90.00° R .03
UP 90.00° R .03
UP 90.00° R .03
UP 90.00° R .03
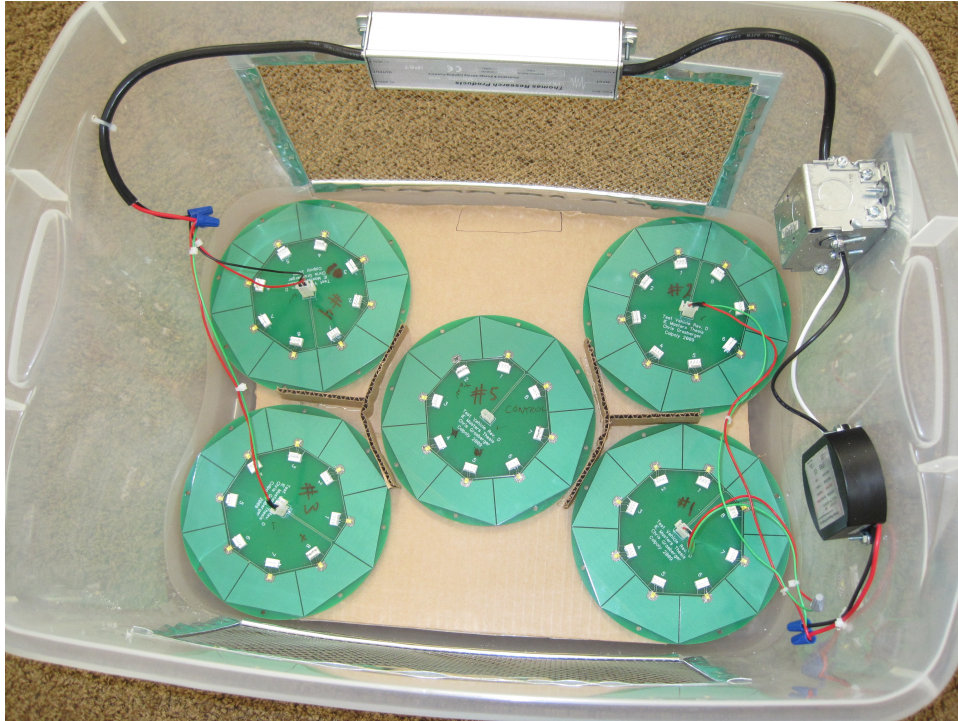UP 90.00° R .03
5.68
4.25
6.12
2.12
.68
.25
35.38
.38
41.64
42.70
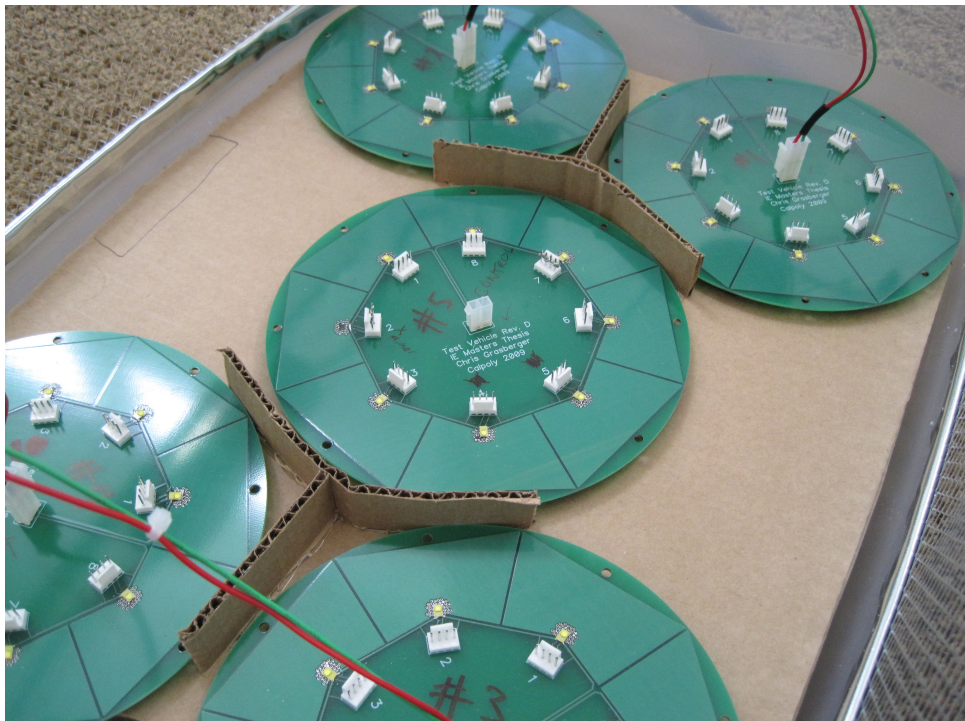
85

Appendix B – Test Environment

Box built to protect LEDs during aging

Close up of a test vehicle with 8 LEDs

Air vent in test box to circulate air

Test groups at both ends of the box with the control in the center